Journal of Nuclear Materials 380 (2008) 126–143

Contents lists available at ScienceDirect

Journal of Nuclear Materials

journal homepage: www.elsevier.com/locate/jnucmat

Review

Overview of experimental programs on core melt progression and fission product release behaviour

B.J. Lewis [a,*], R. Dickson [b], F.C. Iglesias [c], G. Ducros [d], T. Kudo [e]

[a] Royal Military College of Canada, P.O. Box 17000, Kingston, Ontario, Canada K7K 7B4
[b] Atomic Energy of Canada Limited, Chalk River Laboratories, Chalk River, Ontario, Canada K0J 1J0
[c] Candesco Corporation, 230 Richmond Street, 10th Floor, Toronto, Ontario, Canada M5V 1V6
[d] Commissariat à l'Energie Atomique, CEA Cadarache, Building 315, BP 01, 13108 Saint Paul lez Durance, France
[e] Japan Atomic Energy Agency, 2-4 Shirakata-Shirane, Tokai-mura, Ibaraki-ken 319-1195, Japan

ARTICLE INFO

Article history:
Received 23 May 2008
Accepted 14 July 2008

ABSTRACT

An overview of experimental programs that have been conducted to better understand core melt progression phenomena and fission product behaviour during severe reactor accidents in light water reactors is presented. This discussion principally focuses on the melting and liquefaction of core materials at different temperatures, materials oxidation and relocation, hydrogen generation behaviour, and the release and transport of fission products and aerosols. A comparison of fission product release results from annealing and in-reactor experiments is also presented.

Contents

1. Introduction

Numerous in-pile [1–27] and out-of-pile experiments [28–39] have been conducted to better understand light water reactor (LWR) severe accident progression following the accident at the Three Mile Island Unit 2 (TMI-2) nuclear power plant. These experiments have principally focused on high temperature core melt progression and fission product release behaviour. Specifically, the experiments were designed to investigate: (i) how the core loses its original geometry as a result of interactions between core materials and fuel liquefaction; (ii) the relocation behaviour of the core with melt formation leading to partial core blockage, fuel debris beds and molten pools; (iii) how much hydrogen is produced by the steam oxidation of core materials with relocation; (iv) the influence of core degradation on the release, transport and deposition of fission products and aerosols; and (v) the fragmentation of the degraded core with cool down and/or quenching [40–49].

This paper reviews previous separate-effects and integral-effects experiments conducted to better understand core melt progression phenomena (see Section 2). The understanding and experience gained in these various experiments for core melt phenomena (Section 3) and fission product release behaviour (Section 4) are discussed and compared. This discussion is also presented in light of the phenomena inferred from examination of the damaged TMI-2 reactor core [16].

* Corresponding author. Tel.: +1 613 541 6611; fax: +1 613 542 9489.
E-mail address: lewis_b@rmc.ca (B.J. Lewis).

0022-3115/$ - see front matter © 2008 Elsevier B.V. All rights reserved.
doi:10.1016/j.jnucmat.2008.07.005

2. Review of melt progression and fission product release experiments

Table 1 provides a summary of in-pile and out-pile experiments used to investigate core melt progression phenomena and fission product release behaviour during severe accident conditions. The in-pile experiments include: the source term experiments project (STEP), the annular core research reactor (ACRR) source term (ST) tests, the ACRR damaged fuel (DF) relocation experiment, the power burst facility (PBF) severe fuel damage (SFD) tests, the full-length high temperature (FLHT) tests, the loss-of-fluid test facility (LOFT) fission product (FP) test, and the Phebus fission product (FP) and severe fuel damage (SFD) tests. The out-of-pile experiments include: the CORA, QUENCH and CODEX integral programs, and annealing experiments conducted at the Oak Ridge National Laboratories (ORNL) (i.e., the horizontal induction (HI) and vertical induction (VI) test series), Commissariat à l'Energie Atomique (CEA) (i.e., the Heva and Vercors test series) and the verification experiments of radionuclides gas/aerosol release (VEGA) program at the Japan Atomic Energy Agency (JAEA).

Various sizes of bundles (see Fig. 1) were used in the fuel-degradation experiments. The bundles varied from four rods to up to 100 rods with rod lengths between 0.15 and 4 m. The experiments were carried out without fuel irradiation, as well as over a wide range of fuel burnups from trace irradiation to commercial burnup conditions of up to 70 GWd/tU. The effect of system pressure from ~0.2 to 8 MPa on bundle degradation was considered. The steam flows spanned steam-limited to steam-rich conditions to determine how such flows affect the oxidation behaviour of the fuel rod and structural materials and the hydrogen generation behaviour. Different heating methods were employed including: internal electrical heaters, annealing furnaces, fission heating and decay heat. Structural materials (i.e., Inconel and Zircaloy spacer grids) and absorber materials (i.e., Ag–In–Cd or B_4C control rods within Stainless Steel tubes or blades) were also used in the in-pile experiments to investigate their effect on the core meltdown progression and aerosol production.

In-pile tests provided data on core melt progression and fission product release behaviour. The STEP experiments were designed to principally focus on fission product and aerosol chemistry. The ST tests were separate-effects experiments to study fission product and aerosol release from highly irradiated fuel in a reducing atmosphere (hydrogen–inert gas mixture). The DF tests investigated the effect of coolant flow rate, system-fuel rod relative pressure and degree of initial cladding oxidation on the core damage. The SFD tests examined fuel bundle behaviour, hydrogen generation, and the release, transport and deposition of fission products. The FLHT tests studied oxidation and hydrogen generation in full-length rods. The LOFT FP-2 test was a relatively large experiment to determine fission product transport and the effect of steam supply and reflood for a severely damaged core assembly. The Phebus FP experiments simulate the core, cooling system and containment response for a severe accident, including the fission product release, transport and (long term) deposition behaviour. The out-of-pile CORA test matrix focused on the temporal behaviour of core melt progression and reflood characteristics, using electrically heated and instrumented rods. The annealing experiments, conducted at the ORNL (HI and VI tests) and CEA (HEVA and VERCORS tests), were principally designed to investigate fission product release from spent fuel under various atmospheric conditions (i.e., hydrogen, steam and air). In addition, the VEGA annealing tests at JAERI investigated oxidation, dissolution and fission product release behaviour for pressurized water reactor (PWR), boiling water reactor (BWR) and mixed oxide (MOX) fuels at high temperatures in helium and helium/steam mixtures at pressures of 0.1 and 1.0 MPa [39].

The in-pile Phebus Fission Product (Phebus FP) program is detailed in Table 2 and consists of five in-pile tests to study the early phase behaviour of in-vessel core melt degradation over various atmospheric (i.e., oxidizing and reducing) conditions and system pressures (0.5–3.5 MPa) in a temperature range up to 2800 K [50]. For instance, the first two Phebus FP experiments were designed to provide information on the differences between the degradation of fresh (FPT-0) and irradiated (FPT-1) fuel rods (see Tables 1 and 2) for a low-pressure transient (~0.2 MPa) [20,21]. The FPT-4 test was performed to investigate semi-volatile fission product and actinide release from a UO_2/ZrO_2 rubble bed. Except for FPT4 each of these tests employed 21 PWR fuel rods with bundles of 0.8 m in active length. The objective of this program was to investigate severe accident phenomena and fission product release and transport in the core, primary circuit and containment. These experiments specifically provide information on: (i) core melt progression, and materials oxidation and hydrogen generation; (ii) release of volatile fission products from overheated/liquefied fuel and their interaction with structural material aerosols; (ii) aerosol depletion in the primary circuit and containment (including iodine re-volatilization effects in containment); and (iii) the influence of condensation, pool boiling and containment sprays on the source term [17]. The facility is also designed so that it is a 1/5000 reduction of scale of the primary circuit and containment building of an actual pressurized water reactor. This facility therefore offers several advantages, compared to the other in-pile facilities in Table 1, which include: a complete integral design (including a simulated primary circuit and containment vessel); complete instrumentation to assess the temporal and spatial progression of the core melt sequence, including on-line and sequential sampling of solid, liquid and gaseous effluents at various points in the experimental train (e.g., fission product, aerosol and iodine speciation sampling); the possibility of conducting the experiment over extended periods of time (at high temperature); and complete pre and post-test examination (including gamma scanning, and transmission and emission tomography). The data obtained from this program, as well as the out-of-pile Vercors program, have been extensively used for verification of codes for source term analyses [25,27,51–53].

Other experiments not included in Table 1 include Melt Progression MP-1 and MP-2 tests that were also conducted in the ACRR reactor [54,55]. These experiments address the basic mechanisms involved in the behaviour of ceramic melt pools in blocked core accidents as occurred in the TMI-2 accident. The MP experiments demonstrate the growth of a ceramic pool in a pre-formed particulate ceramic (UO_2–ZrO_2) debris bed, which was supported by a pre-cast metallic crust across 32 clad fresh-rod stubs in an inert helium environment. The QUENCH program [56] used arrays of 21 fuel element simulators containing ZrO_2 pellets in a follow on of the CORA program to study the consequences of reflooding and cooling of a degraded core [57]. The CODEX program [58,59] used arrays of seven or nine fuel element simulators containing UO_2 pellets and tungsten bar heaters to investigate reflooding and air oxidation behaviour. The CODEX simulators were clad with Zr–1% Nb when used in VVER configuration, and with Zircaloy-4 when used in PWR configuration.

In-reactor tests of CANDU fuel and fission product behaviour under accident conditions were also performed in the Blowdown Test Facility (BTF) program in Canada. In the BTF-107 experiment, a three-element cluster of CANDU-sized fuel elements was subjected to severely degraded cooling conditions resulting in a high temperature ($\geqslant$2770 K) transient [60,61]. A flow blockage developed during the test due to relocation of U–Zr–O alloy and the high temperature transient was terminated with a cold water quench. The other three experiments in the BTF program, BTF-104, BTF-105A and BTF-105B, were conducted with single CANDU-sized fuel

Table 1
Summary of single-effect and integral LWR severe accident tests[a]

Test or accident	Burnup (GWd/tU)	Control materials	Spacer grids	Maximum temp. (K)	Steam input (g/s)	Atmosphere	No. rods/length (m)	Heating method	Pressure (MPa)	Reference
In-pile tests										
STEP-1	33–36	None	None	2900	Limited	Steam	4/1.0	Fission	0.32	[1]
STEP-2	31	None	None	2600	Limited	Steam	4/1.0	Fission	0.16–1.24	[1]
STEP-3	36	None	None	2200	Limited	Steam	4/1.0	Fission	8.00	[1]
STEP-4	36	Ag–In–Cd	None	2200	Limited	Steam	4/1.0	Fission	7.86	[1]
ACRR ST-1	47	None	None	2450	None	Argon/H_2	4/0.15	Fission	0.16	[2]
ACRR ST-2	47	None	None	2450	None	Argon/H_2	4/0.15	Fission	1.9	[2]
ACRR DF-1	Trace	None	Inconel		Limited	Steam	9/0.5	Fission	0.28	[3]
ACRR DF-2	Trace	None	Inconel		Limited	Steam	9/0.5	Fission	1.72	[4]
ACRR DF-3	Trace	Ag–In–Cd	Inconel		Limited	Steam	8/0.5	Fission	0.62	[4]
ACRR DF-4	Trace	B_4C	Inconel	2700	Limited (0.88)	Steam	14/0.5	Fission	0.69	[5]
PBF SFD-ST	Trace	None	Inconel	2800	Excess (16)	Steam	32/0.9	Fission	6.9	[6]
PBF SFD 1-1	Trace	None	Inconel	2800	Limited (0.7–1.0)	Steam	32/0.9	Fission	6.8	[7]
PBF SFD 1-3	35–42	None	Inconel	2800	Limited (0.6–2.4)	Steam	28/1.0	Fission	6.85 and 4.7	[8]
PBF SFD 1-4	29–42	Ag–In–Cd	Inconel	2800	Limited (0.6–1.3)	Steam	28/1.0	Fission	6.95	[9,10]
FLHT-1	Trace	None	Inconel		Excess	Steam	12/4.0	Fission	1.38	[11]
FLHT-2	Trace	None	Inconel		Limited (1.4)	Steam	12/4.0	Fission	1.38	[12]
FLHT-4	Trace to 28	None	Inconel	2500	Limited (1.26)	Steam	12/4.0	Fission	1.38	[13]
FLHT-5	Trace to 28	None	Inconel + Zircaloy	2600	Limited (1.23)	Steam	12/4.0	Fission	1.38	[14]
LOFT FP-2	0.45	Ag–In–Cd + H_3BO_3	Inconel	2800	Excess (180)	Steam	100/1.7	Decay	1.1	[15]
TMI-2	3	Ag–In–Cd + H_3BO_3	Inconel	2800	Excess	Steam	36816/4.0	Decay	5–15	[16]
FPT-0	Trace	Ag–In–Cd	Zircaloy	~2870[d]	Limited (0.5–3.0)	Steam	20/1.0	Fission	0.2	[20]
FPT-1	23.4	Ag–In–Cd	Zircaloy	2500[d]	Limited (0.5–2.2)	Steam	20/1.0	Fission	0.2	[21]
Out-of-pile tests										
CORA[b]	None	Ag–In–Cd/B_4C	Inconel + Zircaloy	$\leqslant$2200–2700	Variable (2–12)	Steam	25–57/1.0	Electric	0.2–1.0	[28,29]
HI 1–6	10–40	None	None	1675–2275	(8–500) $\times$ 10^{-6}	Steam	1/0.15–0.20	Anneal	0.1	[30]
VI 1–7	40–47	None	None	2000–2700	0–0.021	Steam/H_2/air	1/0.15–0.20	Anneal	0.1	[31]
HEVA 1–8	19–37	None[c]	None	1900–2370	0–0.10	Steam/H_2	1/0.080	Anneal	0.1	[32]
VERCORS 1–6,	38–55	None	None	2130–2620	0–0.025	Steam/H_2	1/0.080–0.087	Anneal	0.1	[33]
HT 1-3, RT 1–8	39–70	None/Ag–In–Cd/Boric oxide	None	2970–fuel melting	Variable	Steam/H_2/air	1/0.080	Anneal	0.1	[37]
VEGA 1–8, M1, M2	43–56	None	None	2770–3120	Variable	Helium/steam	1/0.020	Anneal	0.1 or 1	[38,39]

[a] Adapted from Refs. [10,33,42,43].
[b] The CORA test matrix includes 19 tests.
[c] HEVA 7 had an Ag–In–Cd control rod exclusively, and HEVA 8 had both control rod and fuel materials.
[d] The temperatures for the Phebus FPT-0 and FPT-1 tests correspond to the maximum measured temperatures during the oxidative phase. The quoted value for Phebus FPT-1 is also close to that estimated for fuel relocation during the heatup phase. It is likely, however, that higher temperatures (>2800 K) were reached in the molten pool of these tests.

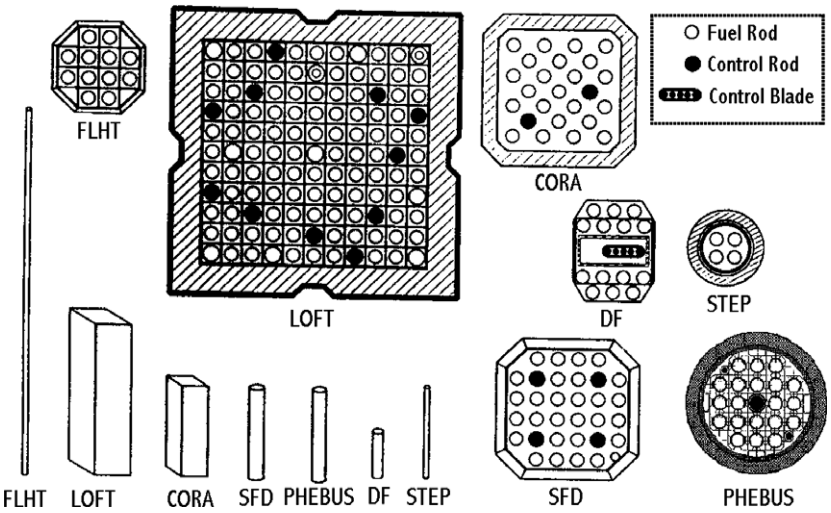

Fig. 1. Bundle configurations and relative scale (adapted from Ref. [42]).

elements at maximum temperatures of 1800–2200 K in a steam-rich environment (~5 g/s steam supply flow). The BTF-104 experiment provided data on fuel behaviour, and volatile fission product release and transport (Kr, Xe, I, Cs, Te and Ba) from a previously irradiated fuel element at a fuel temperature of about 1800 K [62–64]. The primary objectives of the BTF-105A experiment were to obtain data for validation of transient fuel performance codes and to test instrumentation for the BTF-105B experiment [65,66]. The BTF-105B experiment had thermalhydraulic boundary conditions which were better quantified and was performed to investigate fission product release and transport from a previously irradiated fuel element at a fuel temperature of 2100 K [67,68].

In addition to the in-pile experiments, a further summary of the major out-of-pile annealing test programs is further presented in Section 2.1. Results from the various in-pile and out-of-pile experiments are compared to both core samples taken from the TMI-2 reactor and an extensive analytical analysis of the reactor accident (Section 3).

2.1. Single-effects (out-of-pile) fission product release experiments

As shown in Table 1, extensive single-effects annealing tests have been conducted at the ORNL in the United States of America (Section 2.1.1), the Commissariat à l'Energie Atomique (CEA-Grenoble) in France (Section 2.1.2), the JAEA in Japan (Section 2.1.3), and the Chalk River Laboratories (CRL) of Atomic Energy of Canada Limited (AECL) in Canada (Section 2.1.4). These tests were designed to investigate the release behaviour of fission products in high temperature accidents with variable atmospheric conditions.

2.1.1. ORNL experiments

Important tests conducted at the ORNL include the HI and VI series [30,31], as detailed in Tables 3 and 4, respectively. Zircaloy-clad UO_2 fuel samples 15–20 cm long (100–200 g) and irradiated to typical LWR burnups were used in these tests. The fuel specimens were heated under atmospheric pressure up to 1700–2700 K using induction furnaces where the time at temperature varied from 2 to 60 min. Major differences between the VI and HI tests were that: (i) the VI tests were oriented vertically whereas the HI test were horizontal; (ii) the fuel burnups in the VI tests were for the most part higher than those used in the HI tests; and (iii) VI test temperatures (2300–2700 K) were higher than HI test temperatures (1675–2275 K). The VI-3, VI-5 and VI-6 tests were performed at maximum test temperatures of approximately 2700 K; the test atmosphere (steam in VI-3, hydrogen in VI-5, hydrogen followed by steam in VI-6, and air and steam in VI-7) was varied so that the influence of the atmosphere on the fission product release could be studied.

Measurements made in these tests included: (i) test sample temperature versus time by optical pyrometry; (ii) thermal gradient tube measurements downstream of the fuel sample to collect condensing vapors; (iii) use of graduated filters and impregnated charcoal cartridges to collect particulates and volatile iodine species; (iv) a charcoal cold trap to collect and measure fission gases; and (v) radiation detector measurements to monitor fuel location and provide on-line measurements of cesium species in the thermal gradient tubes and Kr-85 in the gas traps. All test components were also sampled and analyzed by gamma-ray spectrometry neutron activation analysis, spark-source mass spectrometry, and emission spectrometry after each test. These tests showed similar release rates for noble gases, Cs and I; however, a difference in transport behaviour was noted for Cs in steam relative to hydrogen. Reactive vapor forms of Cs predominate in hydrogen conditions, while transportable aerosols were noted in steam conditions. The releases of Te and Sb appear to occur from the UO_2 at fractional release rates similar to those for the volatile fission products, but these elements are retained by metallic Zircaloy so their release is delayed until cladding oxidation is nearly complete. Both Eu and Sb showed a sensitivity to the oxygen potential at high temperature [31]. Sb release rates were observed to increase in steam conditions relative to hydrogen at higher temperatures while hydrogen-rich conditions caused higher releases of Eu compared with steam environments [69].

There was limited on-line measurements of fission product release rates (only Cs-137 and Kr-85). Since a segmented furnace tube was used in the tests to allow for rapid heating, there was not good containment of the test environment and there is evidence of oxidation of the graphite susceptor in some tests [34]. The samples were typically at temperature for a relatively short period of time (about 20 min), which may not have been long enough to see oxidative releases, especially at lower temperature.

2.1.2. CEA-Grenoble experiments

Fission product and structural material releases from PWR fuel specimens have been studied in out-reactor experiments by the CEA-Grenoble [32–37]. The HEVA program was conducted be-

Table 2
PHEBUS FP test matrix[a]

Test no.	System pressure	Fuel bundle		Primary circuit	Containment vessel	Comments
		Burnup (GWd/tU)	Sweep gas H_2/H_2O ratio			
FPT-0 (December 1993)	Low	Fresh + P/C[b] (~9 d)	Low	Steam generator (SG), no steam condensation	Closed, pH 5, buffered	First test with fresh fuel (~50% liquefied fuel, >80% volatile FPR[c])
FPT-1 (July 1996)	Low	23 + P/C (~7.4 d)	Low	Same as FPT-0	As FPT-0 but with higher humidity	Previously irradiated fuel with conditions similar to FPT-0 (~20% liquefied fuel, ~70–80% volatile FPR)
FPT-4 (July 1999)	Low	33	Low	Filter package in the in-pile section	Vessel not used	Investigated semi-volatile FP and actinide release from UO_2/ZrO_2 rubble bed
FPT-2 (October 2000)	Low	32 + P/C	High	Same as FPT-0 with boric acid aerosols	As FPT-1 but with sump evaporation and pH 9	Similar to FPT-1 but conducted under steam-starved conditions with boric acid injection
FPT-3 (November 2004)	Low	23 + P/C	High	Same as FPT-0	pH 5, evaporating sump, hydrogen recombiner coupons	Stainless steel clad B_4C control rod

[a] Adapted from Ref. [19].
[b] P/C = pre-conditioned by irradiation in the Phebus reactor prior to the test to restore the short-lived fission product inventory.
[c] FPR = Fission product release.

tween 1983 and 1989, and consisted of 8 tests in the temperature range 1900–2370 K. An induction furnace was used to heat Zircaloy-clad specimens of PWR fuel, and gamma spectrometry was used to measure the fission product releases from the fuel and transport to different locations in the apparatus. In most of the tests, aerosols were collected in a heated cascade impactor and in filters. The temperature of the impactor was varied in the HEVA tests (but not in the VERCORS test series). Control rod materials were used in the last two tests (HEVA-07 with Ag–In–Cd exclusively and HEVA-08 with both control rods and fuel). Mixtures of steam/H_2 and pure H_2 have been used as the environments for the HEVA tests. Table 5 details the HEVA test conditions and fission product release results.

The VERCORS program was an extension of the HEVA tests from 1989 to 1994 using a modified apparatus and augmented instrumentation. The fuel sample consisted of three spent PWR pellets with two half pellets of depleted uranium placed at either end which were held in place by crimping the cladding so that the fuel specimens were not fully sealed. In most of the more recent tests in the HEVA-VERCORS program, the fuel specimens were re-irradiated in the SILOE or OSIRIS research reactors after a period of decay following discharge from the power reactor, which permits detection of short-lived fission products such as I, Te, Mo, Ba and La. Six tests were completed in the VERCORS program to study volatile and semi-volatile fission product behaviour up to a maximum temperature of 2620 K. Extensive post-test gamma scanning (including gamma tomography) were completed after each test. Test conditions and results from the VERCORS test series are detailed in Table 6.

Post-test gamma scanning enabled a complete fission product mass balance. The VERCORS program confirmed a nearly total release of such volatile species as Cs, I, Te and Sb. Their release kinetics are very sensitive to the environment oxygen potential, however, the Te and Sb fission product were observed to be trapped in the unoxidized cladding although their level of release eventually reached that of the other volatiles. Furthermore, their release kinetics is also sensitive to fuel type (UO_2, MOX) and burnup. The semi-volatile fission products included Mo, Pd, Tc, Rh and Ba, whose chemical forms inhibit their release to nearly half that of the volatiles, exhibiting a sensitivity to the atmospheric conditions. Interaction between these group members and the sample burnup can affect the release of some of these species. Ba can be trapped by the Zr in the cladding and Mo can react with Cs reducing its volatility. The Mo release was observed to increase in oxidizing conditions (e.g., 92% release in VERCORS 5 versus only 47% in VERCORS 4) while, in contrast, Ba and Rh releases increased in reducing conditions (e.g., 45% and 80% of Rh and Ba, respectively, in VERCORS 4 as compared with only 20% and 55% in VERCORS 5). The low-volatile fission product and actinide species consisted of Ru, Nb, Sr, Y, La, Ce, Eu, U, Np, and Pu with releases generally between a few and 10%. An increase in sample burnup was shown to enhance the release of some members of this group. Also, their releases are sensitive to the environmental oxygen potential despite the observation of no clear enhancement in release for Np, Ce and Ru (VERCORS 4 and 5). Ru releases are known to be significantly enhanced in air [70].

There was no significant releases of the non-volatile fission products of Zr, Nd and Pr under the temperature range studied in the VERCORS 1-6 experiments. In the VERCORS 6 test performed with high-burnup fuel, although early fuel collapse and partial liquid corium was observed, there was no significant enhancement in release, where the liquid phase retained a fraction of semi- and low-volatile fission products. There were similar problems due to flow bypass in the VERCORS tests as for the ORNL tests with the control of the environment (atmospheric conditions) and measurement of the oxygen potential.

Table 3
ORNL HI-series test conditions and results

Test characteristic	Test number					
	HI-1	HI-2	HI-3	HI-4	HI-5	HI-6
Specimen source, reactor	H.B. Robinson	H.B. Robinson	H.B. Robinson	Peach Bottom 2	Oconee 1	Monticello
Specimen length (mm)	203	203	203	203	152	152
Specimen mass (g)[a]	168	166	167	306	133	170
Fuel burnup (GWd/MgU)	28.1	28.1	25.2	10.1	38.3	40.3
In-pile gas release (%)	0.3	0.3	0.3	10.2	4.1	2
Steam flow rate (g/h)	0.81	0.76	0.31	0.29	0.03	1.7[b]
Test heatup rate (K/s)	1.2	1.3	2.1	2.3	1.1	2.3
Test temperature (K)	1675	2000	2275	2200	2025	2250
Effective time at test temperature (min)[c]	33.8	22.5	21.3	21.6	21.5	2.5
UO_2 grain size (μm)						
Pre-test	2.8	2.8	2.8	6.6	9.2	–
Post-test	3.4	3.9	4.3	6.6	8.9	–
Fuel-cladding interaction	None	Minor	Yes	Yes	Minor	Yes
Fission product release (% of inventory)						
Kr-85[d]	3.13	51.8	59.3	31.3	19.9	31.6
I-129						
Cs-137	2.04	53.0	35.4	24.7	22.4	24.7
Ag-110m[e]	1.75	50.5	58.8	31.7	20.3	33.1
Sb-125[f]	~0.3	2.9	0.02	>0.09	18.0	6
Te (elemental)[g]	0.02	1.55	>0.001	0.01	0.33	0.06
Ba	~0.25	~0.5	~0.3	<0.4	–	–
Sr	~0.008	–	–	<0.4	~0.08	–
Eu-154	<0.002	–	–	<0.005	–	–
Mo	–	–	–	<0.6	~0.02	–
Sn (clad)	–	~5.9	–	–	–	–
Zr (clad)	–	–	~1.7	~1.1	~0.5	–
La	~0.006	~0.002	~0.0001	~0.0016	–	–
	~0.023	–	<0.0002	–	–	–

[a] Total of UO_2 and Zircaloy.
[b] Average value over test time (rate varied from 0.2 to 2.4 g/min during test).
[c] Includes estimates for heatup and cooldown effects.
[d] Includes Kr-85 released during operation.
[e] Ag-110m data for tests HI-2 through HI-4 are probably low.
[f] Sb-125 are probably biased low for all tests.
[g] Determined by chemical analysis.

Table 4
ORNL VI-series test conditions and results

Test characteristic	Test number						
	VI-1	VI-2	VI-3	VI-4	VI-5	VI-6	VI-7
Specimen source, reactor	Oconee 1	BR3	BR3	BR3	BR3	BR3	Monticello
Fuel burnup (GWd/MgU)	40	44	44	47	42	42	40
In-pile Kr release (%)	0.7	~2	0.3	~5	~2	~2	~2
Test temperature (K)	2020, 2300[a]	2300	2000, 2700[a]	2440	2000,2720[a]	2310	2025, 2310[a]
Effective time at test temperature (min)	20,20	60	20, 50	20	20, 20	60	20,20
Atmosphere							
Fission product release (% of inventory)	Steam	Steam	Steam	Steam	Hydrogen	Hydrogen, steam[c]	Air, steam
Cs-137	63	67	100	96	100	80	71
Kr-85							
I-129	57	31	100	85	100	75	69
Sb-125	37	33	[b]	71	74	67	[b]
Eu-154	33	68	99	6.4	18	64	52
Ru-106	0	0	~0.01	19	57	14	0.04
Te (elemental)	0	0	5.0	0	0	0	[b]
Sr (elemental)	–	–	99	–	82	63	–
Ba (elemental)	–	–	3	–	34	6	1
Sn (clad)	–	19	30	27	76	33	4
Mo (elemental)	–	94	76	0.63	–	–	–
Ce-144	43	86	77	6.9	2.3	12.6	–
	–	–	<0.2	–	2.0	–	–

[a] Test was conducted in two phases at two different temperatures.
[b] Analysis incomplete.
[c] Test VI-6 was heated at 2300 K in hydrogen, then switched to a steam atmosphere.

From 1996 to 2002, the VERCORS (High Temperature) HT and RT (Release of Transuranics) program in Table 7 was carried out to improve the database and to study the release of fission products and actinides during the later phase of an accident with the

Table 5
CEA-Grenoble HEVA series test conditions and results

Test characteristic	Test number							
	HEVA-1	HEVA-2	HEVA-3	HEVA-4	HEVA-5	HEVA-6	HEVA-7	HEVA-8
Specimen source, reactor[a]	CAP/2	CAP/2	BR3	Fes 1/2	Fes 1/2	Fes 1/2		Fes 1/2
Fuel burnup (GWd/MgU)	19.4	19.4	27.7	36.7	36.7	36.7		36.7
Test temperature (K)	1900	2140	2070	2270	2070	2370	2070	2070
Test temperature plateau (s)	900	900	1800	420	5760	1800	1800	600
Flow rate (mg/s)								
H_2	0	0	0.5	0.5	0.5	0.2	0.5	0.5
H_2O	100	30	37	30	30	0	25	25
Fission product release (% of inventory)								
Cs-137	~2	68	38	44	66	30	–	15
I-131	–	–	–	43	62	30	–	12
Xe-135	–	–	–	~42	~65	30	–	–
Te-132	–	–	–	52	54	11	–	5[b]
Sb-125	1	41	20	18	–	0 (Sb127)	–	15[b]
Mo-99	–	–	–	21	55	~4	–	16[b]
Eu-154	–	~15	<3	–	–	~5	–	–
Ce-144	–	9[b]	<3.2	–	–	0 (Ce143)	–	–
Ru-106	–	5[b]	<1.5	–	–	0 (Ru105)	–	–
Ba-140	–	–	–	5.6	–	27	–	6[b]

[a] Reactor: Fes = Fessenheim.
[b] Detection limit.

Table 6
CEA-Grenoble VERCORS series test conditions and results

Test characteristic	Test Number					
	VERCORS-1	VERCORS-2	VERCORS-3	VERCORS-4	VERCORS-5	VERCORS-6
Date of test	11-1989	06-1990	04-1992	06-1993	11-1993	09-1994
Specimen source, reactor	Fessenheim	Bugey	Bugey	Bugey	Bugey	Gravelines
Fuel burnup (GWd/MgU)	42.9	38.3	38.3	28.3	38.3	54.8
Re-irradiation (Siloe)	Yes	Yes	Yes	Yes	Yes	Yes
Test temperature (K)	2130	2150	2570	2570	2570	2620
Test temperature plateau (min)	17	13	15	30	30	30
Atmosphere (end of test)	Mixed $H_2O + H_2$	Mixed $H_2O + H_2$	Mixed $H_2O + H_2$	Hydrogen	Steam	Mixed $H_2O + H_2$
Flow rate (g/min)						
H_2	0.15	1.5	1.5	1.5–0	1.5	1.5
H_2O	0.003	0.027	0.03	0.0123	0	0.03
Time at last plateau (min)	17	13	15		30	30
Fission product release (% of inventory)						
Xenon	33	23	77	86	87	100
Iodine	30	23	70	87	93	97
Cesium	42	30	70	93	93	97
Tellurium	4	18	76	100	>98	97
Antimony	2	7	69	97	98	96
Molybdenum		15	42	47	92	79
Barium	4	4	13	80	55	28
Rhodium			0.52	45	20	4
Yttrium			17			
Strontium				<6	<6	<6
Europium			<6	<5	<3	<4
Ruthenium			0.36	6	6	0.6
Cerium				3	<3	0.2
Neptunium	0.006	0.016	0.4	6	<4	<4
Lanthanum			<4	<3	<3	<3
Niobium						0.3
Uranium[a]				2	2	
Plutonium[a]				0.2	0.2	

[a] Approximate values from ICPOES measurements of aerosols on impactor plates, corrected with ^{137}Cs measurements.

occurrence of fuel liquefaction [36,37]. This program also provided information on the release behaviour of fission products as influenced by the nature of the fuel type (UO_2 versus MOX), the morphology of the fuel (intact pellets versus debris fragments), the effect of fuel burnup, the impact of control materials (Ag, In, Cd and boric oxide) and the influence of the environmental sequence of the accident (oxidizing or reducing conditions). In the more severe VERCORS HT and RT test series, Nb and La have been observed to be released more readily from the fuel. These latter tests also investigated the temperature of fuel collapse, which occurred over a temperature range of 2400–2600 K for fuel burnups of 47–70 GWd/tU, which is about 500 K below the melting temperature of UO_2. The observed differences may be explained by the stoichiometric change of the fuel samples during the tests and maybe the presence of fission products within the fuel matrix.

Table 7
CEA Grenoble VERCORS HT-RT text matrix parameters

Test characteristic	Test Number										
	HT-1	HT-3	HT-2	RT-1	RT-2	RT-5	RT-4	RT-3	RT-7	RT-6	RT-8
Date of test	Jun-996	Jun-2001	Apr-2002	Mar-1998	Apr-1998	Dec-1998	Jun-1999	Nov-1999	Apr-2000	Sep-2002	Nov-2002
Fuel	UO_2	UO_2	UO_2	UO_2	MOX	UO_2	UO_2/ZrO_2 debris bed	UO_2 debris bed	MOX	UO_2	UO_2
Fuel burnup (GWd/tU)	49.4	49.3	47.7	47.3	45.6	61	37.6	39	43	71.8	70
Reirradiation	Siloe	Osiris	Osiris	No	No	Osiris	No	Osiris	Osiris	Osiris	Osiris
Test temperature (K)	2900	2680	2423	2570	2440	~2970	2520	2970	2890	2473	2650
Flow rate (g/min)											
H_2	0.012	0.012	0	0.027	0.027	0.027	0.024	0.075	0.012	0.027	0
H_2O	1.5–0	1.5–0	1.5	1.5	1.5	1.5–0	0.876	0.075	0	1.5	0
Air	0	0	0	0	0	0	0	0	0	0	0.048
Main objective	H_2 atm., high temperature, HT reference test	Boric oxide and SIC injection	Boric oxide and SIC injection	RT reference test	MOX fuel	High burnup	Phebus FPT4 support	Fuel volatil-ization	MOX fuel	High burnup fuel	High burnup fuel/air injection
Fission Product Release (% of inventory)											
Xenon											
Iodine	100										
Cesium	100						>96	100			
Tellerium	100						55	100			
Antimony	100						89	60–95			
Molybdenum	49	33	100	70	53		100	33	7		
Barium	49	85	38				50	93	64		
Paladium				34	42		45	16			
Technetium				21	11		42				
Rhodium							8	7			
Yttrium											
Strontium							1				
Europium	9	11	1				<1.5	~1–2			
Ruthenium	8	6	65	9	5.4		<1.5	~1–2	2	High	high
Cerium	5	0.8	1	3	<3		<1.5	~1–2	14		
Neptunium	7										
Lanthanum	8	13	5								
Zirconium	<3						1	~1			
Niobium	9	18	10					40		High	
Uranium				8	5		10	2			
Plutonium				0.3	0.1		0.1				

In summary, the VERCORS tests have shown that release kinetic of the volatile species is sensitive to the environment oxygen potential, burnup and fuel type.

2.1.3. JAEA experiments

Ten tests have been performed in the VEGA experimental facility [71]. In these tests, the impact on fission product release of temperature, atmosphere, pressure and fuel type were investigated. The experimental apparatus consists of an induction furnace with an associated gas supply system. Sample temperatures were measured by single and dual color pyrometers with an accuracy of ±50 K and the fission product release determined by gamma spectroscopy. Three thermal gradient tubes (TGT), condenser, dryer, cold charcoal trap and hydrogen sensor complete the experimental rig. Gamma spectra from the fuel and charcoal trap were used to determine the fractional release histories of cesium and krypton. The total fractional release was obtained by off-line gamma-ray measurements of the sample before and after the heatup tests. In order to evaluate the released masses of low volatile elements, analyses of the leached acid solution from the piping and filters were performed using ICP-AES and alpha-ray measurement. Test conditions and results from the VEGA test series are detailed in Table 8.

The effect of pressure on the release behaviour in He up to 2773 K was studied [38,72]. These tests showed that the release of Cs at 1.0 MPa was suppressed by about 30% for temperatures below 2773 K compared with that at 0.1 MPa. Consequently, Cs release during high pressure scenarios may be lower than that predicted by current models. Low-volatile species such Eu, Ru and Ce were deposited at or close to the sample location but Cs was transported downstream, where it deposited in the TGT at about 800 K. At the high temperature test, enhanced Cs release rates observed for temperatures above 2800 K were attributed to fuel frothing and melting [73].

The releases from MOX fuel were studied in the VEGA-M1 and M2 tests and their results compared to that from UO_2 [74,75]. Significant Cs releases from MOX fuel were observed at about 1000 K while similar releases were only evident at 1623 K in the UO_2 tests. The variation in Cs release at low temperature is explained by the difference in irradiation history. Despite this difference in the kinetic behaviour, the total Cs releases for both fuel types were similar. In particular, enhanced Cs release rates for temperatures higher that 2800 K observed in UO_2 samples were also evident during the MOX tests. Comparable results were also observed for U, Pu, Sr and Mo for the UO_2 and MOX fuels.

The results of the VEGA tests in steam are consistent with those results at other laboratories [39,76]. Here an increased stochiometric deviation in UO_{2+x} resulted in an enhanced release for the volatiles fission products. In the case of Zircaloy sheathed samples, this effect is absent at temperatures above 2030 K for cases where the sheath metallic phase is present. This observation was attributed to the competing process of urania reduction by molten Zircaloy that controls the stochiometric deviation in this temperature range. Dissolution rates of UO_2 by molten Zircaloy were estimated to be about 1/1000 times lower in steam than in hydrogen environments.

2.1.4. AECL-CRL experiments

Six different types of furnaces have been used in experiments at AECL-CRL, depending on the temperature range and size of specimen. For all experiments, monitoring and control of the gas environment have been a priority in order to determine the oxygen potential of the atmosphere. One of the key features of the AECL program has been on-line measurement of the oxygen potential in the gas stream, which allows for the fuel oxidation kinetics to be calculated [77]. Another key feature of these tests has been a direct measurement of the fission product release rates, using a gamma-ray spectrometer which views the heated specimen through a collimated aperture [78]. A second spectrometer is used to monitor activity in the exhaust gas swept out of the furnace [79].

The fuel specimens include UO_2 fragments (0.2–1.5 g each) that were extracted from irradiated fuel elements after discharge and subsequent cutting. These tests provided information on fission product release from bare UO_2 without any Zircaloy barrier. The role of Zircaloy on fission product release has been investigated using fragments of UO_2 enclosed in Zircaloy foil bags, and short segments of Zircaloy-clad fuel elements with end caps fitted onto the ends of the samples to exclude the surrounding atmosphere from direct contact with the UO_2.

More than 300 annealing tests of fission product release from clad and unclad irradiated fuel samples have been conducted at temperatures from 800 to 2350 K in Ar/H_2, steam and air atmospheres [70,77–86]. Table 9 details the test conditions and key results from a selected number of CRL tests. It has been shown that the presence of the Zircaloy sheath can either inhibit or delay the release of volatile fission products, compared to tests under the same conditions using bare UO_2. The delay is primarily associated with the time required to oxidize the Zircaloy cladding, after which the UO_2 begins to oxidize and cause enhanced release rates. The release rates of volatile fission products from clad fuel samples after complete clad oxidation are almost independent of temperature in the range 1670–2140 K [83]. In more recent experiments with Zircaloy-clad segments, in addition to release from the fuel, deposition and transport of fission products have been studied [87,88]. This work shows that releases of volatile fission products (Kr, Xe, I, Cs and Te) are relatively low in inert or reducing atmospheres but increase significantly after clad oxidation in oxidizing atmospheres. In some of the high temperature tests on unclad fuel samples, large fractions of the UO_2 fuel was volatilized in highly oxidizing environments, leading to releases of low-volatile fission products (e.g., Zr, La, Ba, Ce, Pr, Eu) via a 'matrix stripping' process, where these products are normally soluble in the UO_2 [80,81]. The low-volatile fission products released in hydrogen-rich atmospheres (Eu, Ba, etc.) are different from those released in steam (Mo, Ru, Nb, etc.) due to chemical effects on the fission product volatility. Since the oxygen potential of the environment is known in the CRL tests, it has been possible to develop models for steam and air oxidation of UO_2 [34,81,85]. Significant release of fission products such as Ru and Nb have been observed only in oxidizing environments and after the UO_2 has oxidized to an equilibrium state [86].

3. Degraded core accident phenomena

The important melting and chemical interaction temperatures which result in the formation of liquid phases during severe accident conditions in LWRs are shown in Fig. 2. Depending on the accident sequence, the important physico-chemical material behaviour in pressurized water reactors include [41,47]:

(i) melting of the Ag–In–Cd absorber alloy at ~1073 K (and, on melting of the stainless steel alloy cladding of the control rod at 1720 K, chemical interactions with the Zircaloy guide tube and fuel rod cladding),
(ii) plastic deformation and bursting of the cladding at ~1020–1370 K (depending on the system pressure),
(iii) steam oxidation of structural materials (e.g., stainless steel and Inconel) and fuel rod materials (e.g., Zircaloy and UO_2) at ~1470 K, leading to a rapid temperature escalation and the possibility for fuel rod fragmentation,

Table 8
JAEA VEGA text matrix parameters

Test characteristics	Test number									
	VEGA-1	VEGA-2	VEGA-3	VEGA-4	VEGA-5	VEGA-6	VEGA-7	VEGA-8	VEGA-M1	VEGA-M2
Fuel type	UO_2 (no sheath)	UO_2 (no sheath)	UO_2 (no sheath)	Zircaloy sheath UO_2	UO_2 (no sheath)	Zircaloy sheath UO_2	Zircaloy sheath UO_2	UO_2 (no sheath)	MOX (no sheath)	MOX (no sheath)
Fuel burnup (GWd/MgU)	47	47	47	47	47	56	56	56	43	43
Pu enrichment (wt%)	0	0	0	0	0	0	0	0	5.66	5.66
U enrichment (wt%)	4.1	4.1	4.1	4.1	4.1	4.1	4.1	4.1	0.7	0.7
Irradiation reactor	Takahama 3	Takahama 3	Takahama 3	Takahama 3	Takahama 3 Re-irradiated at NSRR	Fukushima 2 Re-irradiated at JRR-3	Fukushima 2 Re-irradiated at JRR-3	Fukushima 2	ATR Fugen	ATR Fugen
Test temperature (K)	1623 (5 min) 2000 (20 min) 2300 (20 min) 2773 (10 min)	1623 (5 min) 2000 (20 min) 2300 (20 min) 2773 (20 min)	1623 (10 min) 2300 (20 min) 2773 (20 min) 3123 (20 min)	1623 (10 min) 2000 (20 min) 2300 (20 min) 2773 (20 min)	1623 (10 min) 2300 (20 min) 2773 (20 min)	1623 (10 min) 2000 (20 min) 2300 (20 min) 2773 (20 min)	1623 (10 min) 2000 (20 min) 2300 (20 min) 2773 (20 min)	1623 (10 min) 2300 (20 min) 2773 (20 min) 3123 (20 min)	1623 (10 min) 2300 (20 min) 2773 (20 min) 3123 (20 min)	1623 (10 min) 2300 (20 min) 2773 (20 min) 3123 (20 min)
Heat up rate (K/min)	40 (<1623 K) 60 (>1623 K)	40 (<1623 K) 60 (>1623 K)	40 (<1623 K) 60 (>1623 K)	20 (<1623 K) 20 (>1623 K)	40 (<1623 K) 60 (>1623 K)	20 (<1623 K) 20 (>1623 K)	20 (<1623 K) 20 (>1623 K)	40 (<1623 K) 60 (>1623 K)	40 (<1623 K) 60 (>1623 K)	40 (<1623 K) 60 (>1623 K)
Pressure (MPa)	0.1	1	0.1	0.1	1	0.1	1	0.1	0.1	1
Atmosphere (end of test)	He	He	He	Steam/He	He	Steam/He	Steam/He	He	He	He
He (dm^3/min)	1	1	1	1	1	1	1	1	1	1
H_2O (g/min)				0.75		0.75	0.75			
Fission product release (% of inventory)										
Krypton				100						
Iodine						97	97			
Caesium	86	61	100	100	84	93	98	98	97	98
Antimony	89	68	95		67		84		95	96
Ruthenium	5		0	18	0	15	7	0	6	3
Molybdenum								~10	~9	
Strontium								10	2	
Uranium								~1	~2	
Plutonium								2	2.8	

Table 9
CRL selected test conditions and results

Test characteristic	Test number							
	MCE1-1	MCE1-6	MCE1-7	MCE2-13	MCE2-19	HCE2-BM3	HCE2-CM4	UCE12-8
Fuel specimen	Fragment[a]	Fragment	Fragment	Fragment	Fragment	Segment[c]	Segment	Segment
Fuel burnup (MWh/kgU)	257	257	257	457	457	544	457	370
Test temperature (K)	1973	2273	2350	2080	2300	1775	1625	1675
Time at temperature (min)	13	37	17	17	10	110	140	200
Heating rate (K/s)	0.2	0.2	0.2	0.2	0.2	0.1	0.1	0.9
Atmosphere	Air	Ar/2%H_2	Air	Steam	Steam	Steam	Air	Steam
Fission product release (% of inventory)								
Cs-137	80	80	100	92	100	75	75	96
I-131	80	80	100	NA	NA	NA	NA	NA
Nb-95	0	10	45	25	47	<2	3	<1
Zr-95	0	0	30	<2	<2	<2	<1	<1
Ru-103	100	1.0	100	NA	NA	NA	NA	NA
Ru-106	NA[b]	NA	NA	42	80	<2	20	<1
Ba-140	0	40	90	NA	NA	NA	NA	NA
La-140	0	0	35	NA	NA	NA	NA	NA
Ce-144	NA	NA	NA	<5	20	<2	<2	<2

[a] Bare fragment of UO_2.
[b] Isotope was not present in fuel at time of test.
[c] Zircaloy sheathed section of a fuel element (2–5 cm long).

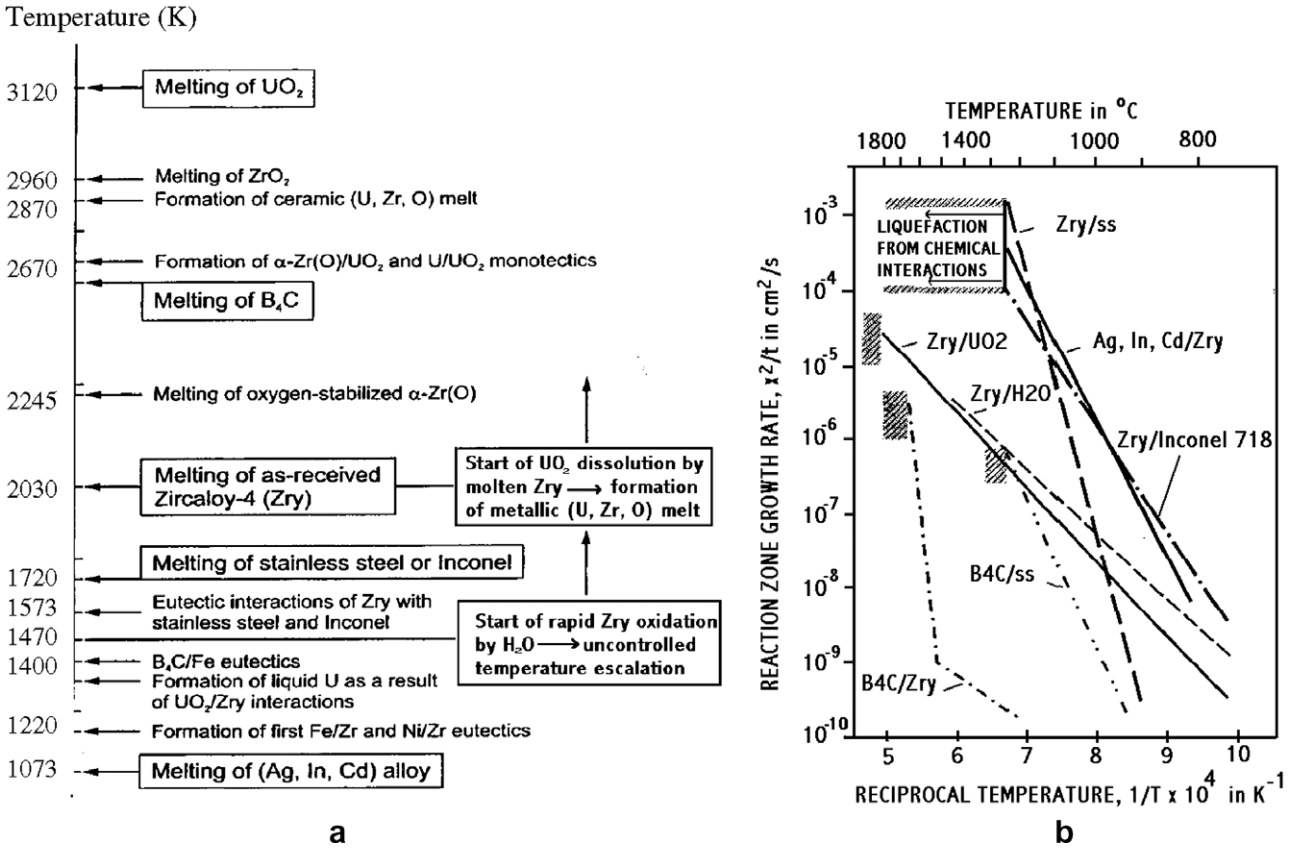

Fig. 2. (a) Severe accident melting and chemical interaction temperatures and (b) growth rates of various reaction couples of reactor material components (Zry = Zircaloy-4 and ss = stainless steel (AISI 316)). (Taken from Ref. [47].)

(iv) eutectic interactions of Zircaloy with stainless steel (e.g., control rod cladding) and/or Inconel (e.g., grid spacers) at 1573 K, interaction of Zircaloy with UO_2 (with hard solid contact) below ~1770 K, and melting of stainless steel or Inconel by ~1720 K,
(v) melting of the as received metallic Zircaloy-4 cladding (2030 K) or the metallic oxygen-stabilized α-Zr(O) phase (2245 K),
(vi) reduction of the UO_2 fuel due to interactions with solid and/or molten metallic Zircaloy (i.e., starting at 2030 K), resulting in a partial dissolution of UO_2 with the formation of a metallic Zr–U–O melt (containing ceramic $(U,Zr)O_{2-x}$ precipitations at higher oxygen concentrations),
(vii) relocation of the liquid and solid materials with formation of immiscible metallic and ceramic melts in different parts of the reactor core (>2030 K),

(viii) melting of the ZrO_2 (2960 K) and UO_2 (3120 K) forming a ceramic melt.

In general, as a consequence of these temperature-dependent phenomena, the core melt will propagate with increasing temperature. It will initiate with the melting of the Ag–In–Cd absorber alloy at ~1073 K. With any localized contact between stainless steel and Zircaloy, liquid phases can form around ~1420–1570 K (initiating liquefaction of both the Inconel grid spacer and absorber rod materials). With failure of the absorber cladding, the molten absorber alloy can come into contact with the Zircaloy of the guide tube and surrounding fuel rods resulting in a chemical destruction of the Zircaloy cladding, and further localized damage as the molten alloy relocates. At temperatures above ~1470 K, the rapid steam oxidation of Zircaloy and stainless steel produces a significant temperature escalation, yielding peak temperatures over 2270 K. When the remaining metallic Zircaloy and/or α-Zr(O) starts to melt (~2030–2270 K), the solid UO_2 may be chemically dissolved and hence liquefied ~1000 K below its melting temperature. Metallic and ceramic melts can then develop and relocate, forming blockages on solidification, which lead to extended core damage. With the melting of the fuel and oxidized cladding from ~2870 to 3120 K, a ceramic melt will form with a complete meltdown of the core itself.

3.1. Comparison of integral experiments

Many of the physical and chemical processes identified in Section 3 have been identified in separate-effects tests, out-of-pile and in-pile integral severe fuel damage experiments, and the TMI-2 core material examinations. All of the integral tests and TMI-2 core examination indicate that the core melt progression is a non-coherent process which takes place over various locations and a considerable period of time. In particular, the small-scale tests that were terminated while melts are still forming and relocating show evidence of multiple melt relocation and oxidation events.

Although various pressures can result depending on the accident scenario, core melt progression phenomena do not vary greatly with pressure as evidenced from the fission-driven experiments (i.e., Phebus FPT-0 and FPT-1 tests were conducted at a relatively low pressure of ~0.2 MPa and the PBF SFD tests near ~7 MPa), the decay-driven LOFT FP-2 experiment (at ~1 MPa), the electrically heated CORA experiments (from ~0.2 to 1 MPa), as well as the TMI accident (with most core damage resulting between 5 and 15 MPa) [42]. In the higher-pressure CORA-9 test (at 1 MPa), no full-length clad collapse was observed, and the flowering behaviour of the fuel rods was not substantially different from the lower-pressure tests [29]. However, ballooning of the cladding and clad failure is enhanced at low pressure where such failure occurred relatively early, even with trace-irradiated fuel, in the Phebus FPT-0 test at ~1008 K. The release of the gap inventory on clad failure was measured in the PBF-SFD tests, LOFT FP-2 test and Phebus FP tests.

Numerous experiments at the Oak Ridge National Laboratory (ORNL) [89], Kernforschungszentrum Karlsuhe (KfK) [29,41,47], UK Atomic Energy Establishment (AEE) Winfrith [90], and Idaho National Engineering Laboratory (INEL) [40] have been conducted to investigate the degradation behaviour of Ag–In–Cd control rods during severe accident conditions. As indicated in Fig. 2(a), the Ag–In–Cd alloy melts between 1070 and 1120 K (i.e., ~800 °C). Although the molten absorber rod alloy is chemically stable with the stainless steel cladding, these experiments indicate that at low system pressures, the control rod can fail as a consequence of localized physical contact between the stainless steel clad and the Zircaloy guide tube, which leads to chemical interaction and a liquid phase around 1420 K [40,47]. Such contact arises from the ballooning of the stainless steel cladding due to the high vapour pressure of cadmium. After failure of the absorber rod cladding, the molten absorber alloy is forcibly ejected from the control rod by the high cadmium vapor pressure [40]. As shown in the CORA tests, this molten material can therefore contact the Zircaloy guide tube and chemically dissolve it, as well as the Zircaloy cladding of the surrounding fuel rods it comes in contact with, well below the melting point of Zircaloy (~2030 K) [29]. In particular, as shown in Fig. 2(b), separate-effects tests have demonstrated that at temperatures greater than 1470 K, the chemical interaction of Ag–In–Cd and Zircaloy will result in a sudden and complete liquefaction [91], with the further possibility of low-temperature UO_2 fuel dissolution. The relocating Ag–In–Cd alloy will therefore propagate and enhance core melt progression at a relatively low temperature. On the other hand, at high system pressures, the control rods with Zircaloy guide tubes will fail at a higher temperature when the stainless steel melting point is reached (~1720 K). In fact, in the low-pressure Phebus tests FPT-0 and FPT-1, the control rod failure occurred at ~1390 K and 1620 K, respectively, (as detected by an activity release of ^{116m}In) below the melting point of the stainless steel as consistent with the low-pressure scenario.

Metallic melts result from interactions of spacer grids, fuel rod cladding and control materials which flow down until a location is reached where the temperature is low enough for solidification to occur forming a partial metallic blockage. Metallic blockages have been observed in earlier in-pile experiments (e.g., PBF SFD 1-1 and 1-4 tests, LOFT FP-2 test, DF-4 test), the out-of-pile CORA tests, the TMI-2 reactor accident and Phebus FP tests. The spacer grid can particularly trap debris if it is at a temperature below the freezing point of the relocating melt [42]. In the PBF SFD experiments and TMI-2 accident, the blockage formed just below the coolant level. On the other hand, in experimental tests where liquid coolant is not present in the bundle (i.e., LOFT FP2, Phebus FP and CORA), such blockages result in the lower (cooler) regions of the bundle. In particular, the freezing temperatures of the melt range from ~1070 K for the Ag–In–Cd alloy to 1220 K for the Zr–Fe eutectic, 1230 K for the Zr–Ni eutectic and elemental silver, 1420 K for the Fe–C eutectic and 1460 K for the Zr–Ag eutectic [42]. The metallic blockages formed in the various integral tests are similar to those formed in the TMI-2 accident but are not as extensive since the experiments were of shorter duration [92]. Silver and alloys of silver and zirconium are found in the lower blockages of the test bundles of the PBF SFD 1-4 test and LOFT FP-2 test, and in the TMI core. Similarly, control rod material has been identified at the bottom of the bundles in the Phebus tests, FPT-0 and FPT-1, frozen in between the fuel rods. Moreover, a post-irradiation metallographic examination of the FPT-0 bundle indicated that the liquid Ag–In material had relocated to the lower part of the bundle, whereas most of the Cd was volatilized on account of its high vapor pressure. The composition of this material, i.e., Zr (20–40 wt%), Ag (10–50 wt%), In (10–40 wt%), U (less than 15 wt%), O (less than 10 wt%) and stainless steel (less than 5 wt%), clearly showed an attack of the Zircaloy cladding by the molten Ag–In–Cd alloy and limited fuel dissolution [20]. These results indicate the role that the control rod plays in the early formation of melts during a reactor accident.

The oxidation of the Zircaloy cladding by steam can result in accelerated heatup rates $\geqslant$10 K/s at temperatures above ~1500–1700 K, depending on steam availability, due to the exothermic nature of the reaction (6.45 kJ/g Zr oxidized). Such heatup rates have been seen in several in-pile tests (e.g., PBF SFD tests and the LOFT FP-2 test) and out-pile tests (e.g., CORA tests) [29,42]. Similar observations were made in the Phebus FP tests. The heatup rate is important since it can influence the in-vessel melt propagation. For

instance, a lower rate of ~1 K/s can permit the solid ZrO_2 layer that is formed during heatup to contain molten Zircaloy, resulting in some UO_2 dissolution, whereas this layer may be too thin at a higher heatup rate (>5 K/s) to contain the molten Zircaloy after which mechanical or chemical breach can result in a relocation of this molten material [47]. Heavy oxidation for instance was observed in the post-irradiation examination near the top of the FPT-0 bundle at ~0.9 m, with the occurrence of significant fuel dissolution by the molten Zircaloy and stainless steel cladding of the absorber rod and upper plug [20].

The majority of the hydrogen generation in the Phebus FPT-0 and FPT-1 tests occurred during the runaway oxidative phase. This result is principally attributed to steam availability. The Zircaloy oxidation and hydrogen generation behaviour observed in the fission-driven experiments (PBF-ST and Phebus FPT-0 and FPT-1) and decay-driven experiments (LOFT FP-2) are compared in Table 10.

More extensive oxidation, and a correspondingly greater degree of hydrogen partitioning before reflood, is noted for the PBF-ST and Phebus FP tests due to the combined effects of a highly steam-rich environment and a relatively longer time available for oxidation during the experiment. A large fraction of the bundle inventory of the LOFT FP-2 bundle was available for subsequent oxidation during reflooding. The latter data demonstrate that significant H_2 generation can be expected during reflooding, which is largely dependent on the degree of prior oxidation and reflood thermalhydraulic conditions. Without the occurrence of a significant Zircaloy oxidation event (and hence exothermic chemical heatup) on reflood, there is also less fission product release on cooldown in the Phebus FP tests compared to that observed in the LOFT FP-2 test. The slightly enhanced fission product release in the Phebus FP tests presumably resulted from molten pool movement with a local heatup of some of the partial fuel rods in the lower bundle locations.

As previously mentioned in Section 3, UO_2 and ZrO_2 are rapidly dissolved by the molten Zircaloy cladding significantly below the melting points of the UO_2 and ZrO_2 (see Fig. 2) [93–101]. For instance, ~45% of the fuel in the TMI-2 core was liquefied in the accident [102], while smaller amounts were observed in the integral tests including 15–18% in the four PBF SFD tests and 15% in the LOFT FP-2 test [42]. The Phebus FP tests, however, were more severe in which ~ 20% of the fuel bundle was liquefied in FPT-1 and up to 50% in FPT-0 [20,21]. This dissolved material is able to relocate downwards to the cooler parts of the core to form channel blockages, i.e., as this material relocates, it is oxidized by the steam and can accumulate more mass with incorporation of solid UO_2 and ZrO_2 debris into the melt. Eventually, ceramic blockages will form at cooler locations, where a separation between this material blockage and the metallic one results since the ceramic $(U,Zr)O_2$ melt freezes at a higher temperature of ~2800 K (and hence higher elevation). The accumulating ceramic material on top of the metallic blockage also has a poorer heat transfer because of the diversion of steam around the blockage and the relatively low thermal conductivity of the ceramic. Consequently, with either decay heating from remaining fission products (e.g., as occurred in the TMI-2 reactor) or increased fission/electrical heating in the integral experiments, the ceramic material will heat up, forming a molten pool within a ceramic crust (see Fig. 3). The smaller accumulations of ceramic melts in most of the integral tests represented earlier stages of molten pool formation. The observed fuel damage in the more severe integral test of Phebus FPT–0 is consistent with that observed in the TMI-2 accident where there is a molten pool under a cavity which is surrounded by a uranium-rich crust (see Fig. 3).

Examination of the formerly molten pool in the TMI-2 core revealed that the pool is principally made of $(U,Zr)O_2$, containing transition metal oxides of Cr_2O_3 and Fe_3O_4in the grain boundaries [103]. The melting point of the pure $(U,Zr)O_2$ ceramic is 2800 K, however, as found in the TMI-2 examination, the transition metal oxides can react eutecticaly with ZrO_2 and lower the liquidus temperature of the ceramic melt by about ~100 K [104]. Similarly, the molten pool of the Phebus FPT-0 test had an average composition of U (62 wt%), Zr (22 wt%) and O (14 wt%), with smaller amounts of Fe (~0.6 wt%) (typically as a second phase inclusion or grain boundary precipitate), and traces of Y and Ce from melt interaction with the shroud [20]. This composition corresponded to $(U_{0.51}, Zr_{0.46}, Fe_{0.03})O_{2\pm x}$ in a $(U,Zr)O_2$ lattice. The melting point of the molten pool in the Phebus FPT-0 test is in good agreement (~2720 K) with that estimated for TMI-2 (~2700 K) [105].

The ceramic crust in the TMI-2 accident failed by thermomechanical loading in which 20 tonnes of melt flowed into the lower plenum (see Fig. 3) [42]. It is also possible during the later stages of a severe accident for the ceramic crust surrounding the pool to thin, weaken and fail although most of the integral tests have been terminated too early during their high temperature phase for such late-phase behaviour to occur. However, in the Phebus FPT-0 test, a downward motion of the molten pool from the lower grid spacer position (i.e., at 0.20–0.30 m) was observed at ~18 100 s [20]. In fact, as evidenced in the destructive examination and chemical analysis, two main mixtures resulted near the bottom of the bundle, corresponding to metallic material from the control rod/cladding interaction and the previous molten ceramic that had also been observed higher up at the lower grid position [20]. At the time of this movement, there was an induced steam redistribution in the external gap of the shroud due to an increased flow blockage, an increase in the lower bundle temperature, an increase in reactivity (due to a possible hafnium movement with the melt mixture to the bottom of the bundle), and an increased aerosol release as detected by the on-line monitoring indicating a mixing of the molten pool with the lower part of the bundle [20]. This behaviour is similar to that observed in the MP experiments [54,55]. In these latter experiments, the ceramic pool is contained by a crust in the ceramic (UO_2-ZrO_2) particulate debris bed with local crust melting and refreezing occurring in the debris bed as the crust and pool grew. Although the ceramic crust in the MP experiments had migrated into the fuel rod stubs, it did not fail.

In the TMI-2 accident, a debris bed was formed on top of the molten pool and in the lower plenum region (see Fig. 3) [16]. An upper debris bed was also observed in the SFD-ST [6] and LOFT FP-2 [106,107] tests when coolant was introduced into the hot bundle, resulting in a thermal shock and fragmentation of the oxidized fuel rods. In less steam-rich transients, however, as seen for example in the SFD 1-4 [9,10] and Phebus FPT tests [20,21], a debris bed in the upper part of the bundle of decladded fuel and

Table 10
Summary of Zircaloy oxidation and hydrogen generation behaviour in various in-pile experiments[a]

Test	Oxidation of Zircaloy (%)	Time (s)	Partitioning of H_2 generation (%)	
			Before reflood	After reflood
LOFT FP-2	49[b]	~300 ($T \geqslant 1700$ K)	20	80
PBF-ST	75[b]	~600 ($T \geqslant 1700$ K)	77	23
Phebus FPT-0	85[c]	~1200[d]	82[e]	—
Phebus FPT-1	68[c]	~900[d]	91[e]	—

[a] Adapted from Ref. [44].
[b] Based on total bundle inventory of Zircaloy cladding, shroud inner liner and Zircaloy guide tubes.
[c] Total bundle zirconium mass not including Zircaloy support plate.
[d] Time duration of the oxidation phase. For FPT-0, the bundle remained over 2200 K for ~6000 s.
[e] Fraction of H_2 generation up to the end of the runaway oxidative phase (~13 000 s for FPT-0 and ~12 000 s for FPT-1).

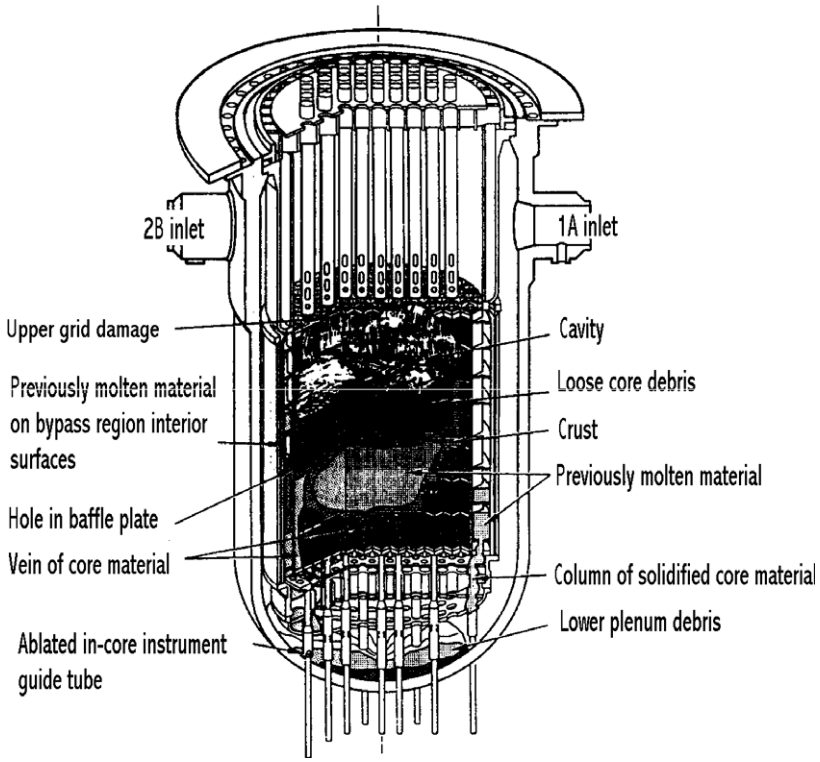

Fig. 3. Schematic of the end-state configuration of the damaged TMI-2 core. (Taken from Refs. [42,92].)

fragments was formed by the melting (as enhanced by interactions from structural and control rod materials) and relocation of the Zircaloy fuel rod cladding.

4. Fission product release behaviour

The fission product release behaviour under severe accident conditions has been reviewed for in-pile (integral-effects) experiments (e.g., ST tests, STEP tests, PBF SFD tests, FLHT tests and LOFT FP-2 test) and the TMI-2 examination [45,92], and more recently for out-of-pile annealing tests (e.g., HI, VI, HEVA, VERCORS, VEGA and annealing experiments at the CRL) used to investigate single-effects behaviour (see, for example, Tables 11 and 12) [35]. The non-coherent nature of the melt progression as detailed in Section 3 generally masks the individual release mechanisms. As such, complementary separate-effects experiments were performed in the out-of-pile Vercors program (i.e., Vercors 1-6 and Vercors HT1-3 and RT 1-8) to provide additional information in order to help interpret the in-reactor results [37].

The fission product releases from the in-pile PBF tests (i.e., SFD-ST (steam-rich), SFD 1-1 (steam-starved) and SFD 1-4 (steam-starved)) and Phebus FPT-1 test (steam-rich) are compared to those in the TMI-2 accident in Table 12. These results indicate very low release fractions for cerium and actinides (typically <0.01%); ruthenium, strontium, and antimony generally less than one percent; barium less than a few percent; molybdenum up to 50%; similar volatile release behaviour of iodine, cesium and noble gases up to ~90%; and tellurium between 1% and 83%. These findings are also consistent with those observed for the annealing experiments in Section 2.1 [35]. However, there is a difference for the barium release between the in-reactor Phebus FPT-0 and FPT-1 experiment (~1%) and the ORNL and VERCORS annealing tests (>40%) (see Tables 11 and 12) [108]. A qualitative thermochemical analysis suggests that this difference may be due to: (i) the short duration of the temperature escalation in the in-pile tests, where there is no 'high temperature plateau' as in the annealing tests but rather a temperature escalation due to the formation of a molten pool in the Phebus experiment; and (ii) the presence of a significant amount of ZrO_2 in the fuel melt (~47 mol%) as well as small amounts of iron oxide in the in-reactor test which can reduce the volatility of Ba [108]. Moreover, thermochemical calculations with the GEMINI2 code specifically suggests that the Ba vapor pressure is reduced in the solidus–liquidus transition zone in the U–Ba–O phase diagram (~2400–3100 K) [108].

As indicated in Table 12, the tellurium release is dependent on the extent of Zircaloy oxidation, where large releases occur when the Zircaloy cladding is nearly completely oxidized. Although tellurium is released from the fuel on heatup, it will chemically react with the Zircaloy cladding and become trapped [109–112]. During Zircaloy oxidation, the tin constituent in the cladding is segregated

Table 11
Conditions and Ba release data for ORNL (HI and VI) and CEA (HEVA, VERCORS and VERCORS HT) annealing tests and Phebus tests[a]

Test	Temperature (K)	Duration (min)	Atmosphere	Ba release (%)
HI-4	2200	20	H_2O	<1
HI-5	2025	23	H_2O	<1
VI-2	2300	60	H_2O	19
VI-3	2700	20	H_2O	30
VI-4	2440	20	H_2	27
VI-5	2720	20	H_2	76
HEVA-4	2270	7	$H_2O + H_2$	6
HEVA-6	2370	30	H_2	27
VERCORS-1	2130	17	$H_2O + H_2$	4
VERCORS-4	2570	30	H_2	80
VERCORS-5	2570	30	H_2O	55
VERCORS HT-1	3070	7	H_2	49
Phebus FPT-0	~2700	–	H_2O/H_2	1
Phebus FPT-1	~2500	–	H_2O/H_2	1

[a] Taken from Refs. [25,108].

Table 12
Comparison of fission product release fractions from in- and out-pile experiments and TMI-2[a]

Element and experimental conditions	Fission product release fractions (%)									
	PBF experiments			Phebus		TMI-2	Annealing ORNL and VI tests			
	SFD-ST	SFD 1-1	SFD 1-4	FPT-0	FTP-1		VI-3	VI-5	VERCORS-4	VERCORS-5
T_{max} (K)	2800	2800	2800	~2870	2500	2800	2700	2720	2570	2570
Atmosphere	H_2O	H_2O	H_2O	H_2O/H_2	H_2O/H_2	H_2O/H_2	H_2O	H_2	H_2	H_2O
Krypton, xenon	50	2.6–9.3	23–52	96	77	54	100	100	86	87
Iodine	51	12	24	100	87	55	79	70	87	93
Cesium	32	9	39–51	84	84	55	100	100	93	93
Tellurium	40	1	3	100	83	6	99	82	100	>98
Barium	1.1	0.6	0.8	1	1		30	76	80	55
Strontium	0.002		0.88			0.1				
Antimony			0.13	62	31	0.16	99	18	97	98
Ruthenium	0.03	0.02	0.007	4	1	0.5	5	0	7	6
Cerium	0.0002	0.009	0.013			0.01				
Europium			0.08			<0.1				
Zirconium/niobium					<1					
Molybdenum				No data	56		77	2	47	92
Actinides			<0.001		<1					
Zirconium oxidized (%)	75[b]	28	38[b]	85	68	45[b]				
Fuel melted (%)	15	16	18	50	20	45				
Test environment	Steam-rich	Steam-starved	Steam-starved	Steam-rich	Steam-rich	Steam-rich	Steam-rich	Steam-starved	Steam-starved	Steam-rich
Fuel burnup (GWd/tU)	Trace	Trace	29–42	Fresh	23	3	44	47	38	38

[a] Adapted from Refs. [25,45].
[b] Test bundle inventory (core inventory for TMI-2) taken from Ref. [44].

as a thin band in the zirconium oxide layer, which advances with the metal/oxide interface, because of its lower solubility in the oxide than in the metal. After complete oxidation, there is a production of elemental tellurium and zirconium oxide from reaction of zirconium telluride with oxygen; however, as a consequence of the tin segregation process, an enhanced formation of SnTe ultimately leads to a release of tellurium. A SnTe compound has in fact been observed by Collins et al. under accident conditions [113]. Only at high oxygen partial pressures, which are above the equilibrium value of Sn/SnO_2, will tellurium be released in its elemental form. This delayed release behaviour for tellurium has been observed in numerous annealing experiments [31,33,35,45,114].

Comparison of the volatile releases in Table 12 for the comparable tests, PBF SFD 1-1 and 1-4, indicate that the release is enhanced in high-burnup fuel compared to trace-irradiated fuel because of the presence of grain boundary tunnels that serve as pathways for gaseous release. Enhanced release rates (due to fuel morphology) occur primarily during the initial heatup, while this difference diminishes afterwards (i.e., above ~2200 K), where releases are now dominated by dissolution of the fuel by the molten Zircaloy cladding [45]. Interestingly, in the Phebus FPT-1 test, the two fresh (instrumented) fuel rods underwent considerably less damage than the 18 irradiated fuel rods [19]. Significant swelling also occurred in the irradiated fuel rods (~22%) but not the fresh fuel rods from the buildup of gaseous fission products. The ST, FLHT and VI tests have shown that significant swelling occur when fuel rods are subjected to high temperature in a reducing environment. The large swelling observed in Phebus FPT-1 implies that similar conditions probably existed during this test.

Release rates of volatile fission products were large during the temperature escalations in the PBF SFD 1-1 and 1-4 tests and the Phebus FPT-0 test. The highest mass flow rates of aerosol and fission products (i.e., ^{131}I, ^{139}Xe, ^{140}Xe, ^{90}Kr and ^{92}Kr), as well as structural materials (such as tin, silver and indium), detected in the Phebus FPT-0 test were observed at about 12 000 s when a peak temperature of ~2770 K was reached at a bundle elevation of 0.7 m. Significant tellurium release also occurred in both Phebus FP tests because of the extent of cladding oxidation. Although antimony like tellurium is readily released from the fuel during heatup in a severe accident, a lower release is observed since the antimony most likely sequesters in metallic melts (as it alloys with other metals such as nickel and silver) [45]. The oxygen potential (dictated by the hydrogen to steam ratio in the gas atmosphere) plays an important role, principally in the release characteristics of the low-volatile fission products [35]. Indeed, only small releases of barium and strontium were observed in the steam experiments of Table 12 as the prevailing atmosphere typically hindered the formation of the more volatile metallic species but favoured low-volatility oxides and hydroxides [115]; in fact, releases for these species occurred in the Phebus FPT-0 test during the temperature escalation phase when hydrogen generation was at a maximum [20]. This observation is consistent with the in-pile ACRR ST experiments, where higher releases of several percent for barium and strontium, and up to 15% for europium, were observed in a reducing environment which would promote higher-volatile metallic forms of these species [2]. These results are also supported by those from the out-of-pile SASCHA experiment at KfK [116], and the VI, HEVA and VERCORS annealing tests [31,33,35]. Since ruthenium has the highest oxygen potential of all fission products, the higher-volatile oxides cannot form for the given steam–hydrogen mixtures of the experiments in Table 12 or in the TMI-2 accident. The formation of uranium-bearing vapor species (e.g., UO_3) depends roughly on the square root of the oxygen partial pressure [115,117]. Fuel release in Table 12 is therefore small for the given conditions of the integral experiments and the TMI-2 accident since only a small amount of hydrogen is required to significantly

lower the oxygen partial pressure, and hence partial pressure of the uranium bearing species.

With the occurrence of fuel liquefaction, the crystal structure of the UO_2 is destroyed so that the release of fission products will be governed by atom and bubble migration in the melt. Although this migration mechanism is faster than diffusion in the solid fuel, a release enhancement is not necessarily observed in the integral tests because of the non-coherent nature of the melt progression. In addition, the fuel and fission product containing liquids will relocate and freeze at lower, cooler elevations, on top of the metallic blockage formed earlier (see Section 3). As seen in TMI-2, the decay heat from fission products trapped in the ceramic blockage can heat up the blockage so that a molten pool can form. The release of fission gases and volatile fission products residing in this molten pool can be further delayed since they must nucleate into bubbles, and then coalescence and grow in the liquid medium by Brownian motion and buoyancy-biased motion, before they can rise by buoyancy to the pool surface for eventual release [34,118,119]. Gas bubbles can also be trapped at the interface between the pool and the crust that surrounds the pool [45]. The oxygen potential of the molten pool will again influence the fission product chemical form, i.e., the presence of iron oxides in the melt of the TMI-2 establishes a lower limit of about −120 kJ/mol at 2800 K so that fission products such as lanthanum, cerium and strontium should exist as an oxide (i.e., La_2O_3, Ce_2O_3 or CeO_2, and SrO) that is soluble in the $(U,Zr)O_2$ ceramic, whereas ruthenium and antimony would be present as metals immiscible in the ceramic melt [45]. Although iodine and cesium are identified as volatile fission products, and should therefore be released through bubble coalescence and buoyancy in molten material, small fractions (3–10%) have been observed in previously molten ceramics in the PBF SFD experiments and the TMI-2 reactor [45]. In agreement with this observation, gamma spectroscopy was able to detect cesium, e.g., ^{134}Cs and ^{137}Cs, (as well as ^{125}Sb and ^{106}Ru) in previously molten material in the Phebus FTP-0 and FPT-1 tests [20,21].

The formation of the molten pool can also result in a flow restriction and a reduced aerosol flow as evidenced in the Phebus FPT-0 test. Fuel movements can significantly affect the dynamics of the aerosol flow and fission product release. Slightly enhanced releases were also observed in the FPT-0 test coincident with the test cool down, as seen for example by the increased activity in containment of ^{132}I, which may be attributed to fuel movement at the end of the test. In comparison, although 3% of the volatile fission product inventory was released in the LOFT FP-2 test during the rapid oxidation transient to 2200 K (i.e., when reflood was initiated), ~12% of the inventory was released during and after reflood [92]. In this case, the reflood with water injection produced a rapid local oxidation of the unoxidized Zircaloy in the upper part of the bundle, and this local heating led to significant fission product release. In the PBF SFD 1-4 test that was conducted with high-burnup fuel rods, the aerosol composition in the upper plenum (at ~600 K) was shown to contain significant percent levels of volatile fission products (i.e., iodine, tellurium and especially cesium) (~25–50%), with the remainder being control rod materials (i.e., silver and cadmium) and structural materials (i.e., tin). As such, the fission product release, vaporization of control materials and release of tin from the oxidized Zircaloy were all important aerosol sources in this experiment [46]. Comparable findings were seen in the Phebus FPT-0 test, except for the significant presence of volatile fission products in the aerosol composition. In particular, a post-test SEM/EDX analysis of aerosol particles collected on the filters and impactors located in the experimental circuit revealed that the particles were composed of mainly thermocouple materials (21–59% of rhenium and 1–10% of tungsten), control rod materials (17–42% of silver, 3–6% of indium and 1–3% of cadmium) and fuel rod materials (7–10% of tin from the oxidized cladding and 1–13% of uranium), with a much smaller amount of fission products (1–2% of molybdenum) [20]. Correspondingly, a similar composition was found in containment with a decreasing mass percent of: Ag (30%), Re (20%), Sn (13%), In (7%), Ni (7%), Cd (6%), U(6%) and a few percent of Fe, Mo and W [20]. In this trace-irradiated test, the mass of the released structural material was several orders of magnitude greater than that of the fission products. A total aerosol mass of 155 g (~1% of the total test bundle mass) was generated and transported through the facility [20]. However, structural materials also played the dominant role in aerosol formation in the Phebus FPT-1 test which used high-burnup fuel. Thus, this result suggests that perhaps the relatively lower fission product content of the aerosols seen in the Phebus FP tests may be a result of a higher silver release as a consequence of the different system pressures between the PBF SFD 1-4 (~7 MPa) and Phebus FP (~0.2 MPa) tests rather than just a burnup effect [105].

5. Conclusions

In-pile and out-pile experimental programs have been reviewed, indicating that melt progression is a non-coherent process as a result of non-homogeneous conditions which exist in the core throughout the transient. The Phebus FPT-0 and -1 tests were performed for a longer period of time at high temperature than earlier in-pile experiments and provide additional information on late-phase behaviour with the presence of irradiated fuel material. Control rod failure leads to a local propagation of the core melt progression at a relatively low temperature. Metallic blockages result from interactions of the spacer grids, fuel rod cladding material and control rod materials that flow down the bundle and solidify at a lower (cooler) position. A separation between the metallic and ceramic blockages arises due to the freezing of the $(U,Zr)O_2$ melt at a higher temperature. The observed melting temperature of the ceramic blockage in the Phebus FPT-0 test (~2720 K) is slightly lower than that of the pure ceramic (~2800 K) due to possible eutectic interaction with the transition metal oxides. This result is consistent, however, with that seen in the TMI-2 examination. As observed in several in-pile experiments, a molten pool is formed which is originally held in place by a ceramic crust. This pool forms due to increased fission heat generation, in which there is a reduced heat transfer due to partial steam blockage from the underlying solidified material and a reduced thermal conductivity in the ceramic. Some molten material relocation was observed to occur in the later phases of the Phebus FP tests. These features are also similar to that observed in the damaged TMI-2 core.

The fission product release behaviour observed in the in-pile and out-of-pile tests has been compared and examined, as well as that determined in the TMI-2 core examination. Consistent release behaviour of the volatile (Xe, Kr, I, Cs, Te and Sb), semi-volatile (Mo, Rh, Ba), low volatile (Ru, Ce, Np, Sr and Eu) and non-volatile (Zr, Nb, La and Nd) fission products was observed in the annealing experiments at the ORNL, CEA, JAEA and CRL and the various in-pile tests except for the release of barium, where a reduced volatility was observed in the in-reactor experiments compared to the annealing tests due to thermochemical effects as a result of the presence of iron and zirconium oxides. It is seen that the prevailing local atmospheric conditions (i.e., oxygen potential) particularly influence the release characteristics of the semi-volatile and low-volatile fission products. Moreover, the non-coherent nature of melt progression tends to mask individual release mechanisms as identified in the out-of-pile experiments. A significant enhancement of release due to fuel liquefaction is not typically observed in the separate-effects experiments.

A slightly elevated release of volatile fission products was observed with termination of the Phebus FPT-1 test; however, this

release was considerably smaller than that observed in the LOFT FP-2 test where a rapid oxidation of the unoxidized Zircaloy (and local heating) followed on reflooding in the latter test. The Phebus FP tests further provided an opportunity to study the long-term aerosol and containment release behaviour, e.g., aerosols in the trace-irradiated Phebus FPT-0 test were principally composed of control rod (Ag, In, Cd), thermocouple (Re) and fuel rod (Sn, U) materials. These aerosol particles contained only minor quantities of fission products (Mo), which contrasted to that found in the earlier PBF SFD 1-4 test where the fission products (I, Te, Cs) had played a more important role in the aerosol formation due to the presence of high-burnup fuel. Only a small fraction of iodine in containment was volatile in the FPT-0 (~2%) and FPT-1 (0.3%) tests.

Acknowledgments

The authors would like to thank L. Dickson (AECL-CRL) for many helpful discussions. The work at the Royal Military College was supported by the Natural Sciences and Engineering Research Council of Canada. The work performed by CEA on the HEVA and VERCORS tests was supported by the French institute for nuclear safety (IRSN) and Electricité de France (Edf).

References

[1] L. Baker Jr., J.K. Fink, R. Simms, B.J. Schlenger, J.E. Herceg, Source Term Experiments Project (STEP): A Summary, NP-5753M, Electric Power Research Institute, March 1988.
[2] M.D. Allen, H.W. Stockman, K.O. Reil, A.J. Grimley, W.J. Camp, in: Proceedings of the International Conference on Thermal Reactor Safety, Avignon, France, 2–7 October 1988, vol. 5, 1988.
[3] R.D. Gasser, C.P. Fryer, R.O. Gauntt, A.C. Marshall, K.O. Reil, K.T. Stalker, Damaged Fuel Relocation Experiment DF-1: Results and Analyses, NUREG/CR-4668, SAND86-1030, US Nuclear Regulatory Commission, January 1990.
[4] K.O. Reil, A.C. Marshall, R.O. Guantt, R.W. Ostensen, P.S. Pickard, C. Fryer, K.T. Stalker, Proceedings of the International Topl. Mtg. Thermal Reactor Safety, San Diego, California, 2–6 February 1986, vol. 3, American Nuclear Society, 1986.
[5] R.O. Gauntt, R.D. Gasser, L.J. Ott, The DF-4 Fuel Damage Experiment in ACRR with a BWR Control Blade and Channel Box, NUREG/CR-4671, SAND86-1443, US Nuclear Regulatory Commission, November 1989.
[6] A.D. Knipe, S.A. Ploger, D.J. Osetek, PBF Severe Ful Damage Scoping Test – Test Results Report, NUREG/CR-4683, US Nuclear Regulatory Commission, March 1986.
[7] Z.R. Martinson, D.A. Petti, B.A. Cook, PBF Severe Fuel Damage Test 1-1 Test Results Report, NUREG/CR-4684, EGG-2463, vol. 1, US Nuclear Regulatory Commission, October 1986.
[8] Z.R. Martinson, M. Gasparini, R.R. Hobbins, D.A. Petti, C.M. Allison, J.K. Hohorst, D.L. Hagrman, K. Vinjamuri, PBF Severe Fuel Damage Test 1-3 Test Results Report, NUREG/CR-5354, EGG-2565, US Nuclear Regulatory Commission, October 1989.
[9] D.A. Petti, Z.R. Martinson, R.R. Hobbins, C.M. Allison, E.R. Carlson, D.L. Hagrman, T.C. Cheng, J.K. Hartwell, K. Vinjamuri, L.J. Seifken, Power Burst Facility (PBF) Severe Fuel Damage Test 1-4 Test Results Report, NUREG/CR-5163, EGG-2542, US Nuclear Regulatory Commission, April 1989.
[10] D.A. Petti, Z.R. Martinson, R.R. Hobbins, D.J. Osetek, Nucl. Technol. 94 (1991) 313.
[11] W.N. Rausch, G.M. Hesson, J.P. Pilger, L.L. King, R.L. Goodman, Coolant Boilaway and Damage Progression Program Data Report: Full-Length High Temperature Experiment 1, PNL-5691, Pacific Northwest Laboratories, September 1986.
[12] N.J. Lombardo, D.D. Lanning, F.E. Panisko, Coolant Boilaway and Damage Progression Program Data Report: Full-Length High Temperature Experiment 2, PNL-6551, Pacific Northwest Laboratories, April 1988.
[13] D.D. Lanning, N.J. Lombardo, D.E. Fitzsimmons, W.K. Hensley, F.E. Panisko, Coolant Boilaway and Damage Progression Program Data Report: Full-Length High Temperature Experiment 4, PNL-6368, Pacific Northwest Laboratories, January 1988.
[14] D.D. Lanning, N.J. Lombardo, D.E. Fitzsimmons, W.K. Hensley, F.E. Panisko, Coolant Boilaway and Damage Progression Program Data Report: Full-Length High Temperature Experiment 5, PNL-6540, Pacific Northwest Laboratories, April 1988.
[15] M.L. Carboneau, V.T. Berta, M.S. Modro, Experiment Analysis and Summary Report for OECD LOFT Project Fission Product Experiment LP-FP-2, OECD LOFT-T-3806, Organization for Economic Cooperation and Development, June 1989.
[16] J.M. Broughton, P. Kuan, D.A. Petti, E.L. Tolman, Nucl. Technol. 87 (1989) 34.
[17] P. von der Hardt, A. Tattegrain, J. Nucl. Mater. 188 (1992) 115.
[18] P. von der Hardt, A. Jones, C. Lecomte, A. Tattegrain, Nucl. Safety 35 (1994) 2.
[19] M. Schwarz, G. Hache, P. von der Hardt, Nucl. Eng. Des. 187 (1999) 47.
[20] N. Hanniet, G. Repetto, Phebus PF, FPT0 - Final Report, CD Version, Suntech 10/99.
[21] J. Bonnin, B. Berthet, S. Bayle, N. Hanniet, F. Jeury, S. Gaillot, Y. Garnier, C. Martin, M. Laurie, B. Siri, Phebus PF, FPT1 - Preliminary Report," IPSN/DRS/SEA/LERES/97/727, Note Technique LERES no. 24/97, Document Phebus PF IP/97/334, October 1997.
[22] M.C. Anselmet, F. Jeury, G. Augier, S. Bayle, R. Berre, S. Bourdon, J.J. Cochaud, B. Cornu, Y. Garnier, J.C. Giacalone, J.M. Girard, G. Gregoire, M. Laurie, J.P. Mahue and E. Ragagli, FPT4 Quick Look Report, Note Technique LEAC 39/99, Note Technique LEMRA 10/99, Document Phebus FP IP/99/453, 21 October 1999.
[23] M. Schwartz, B. Clement, A.V. Jones, Nucl. Eng. Des. 209 (2001) 173.
[24] B. Clément, N. Hanniet-Girault, G. Repetto, D. Jacquemain, A.V. Jones, M.P. Kissane, P. von der Hardt, Nucl. Eng. Des. 226 (2003) 5.
[25] R. Dubourg, H. Faure-Geors, G. Nicaise, M. Barrachin, Nucl. Eng. Des. 235 (2005) 2183.
[26] M.P. Kissane, I. Drosik, Nucl. Eng. Des. 236 (2006) 1210.
[27] L.E. Herranz, M. Vela-García, J. Fontanet, C. López del Prá, Nucl. Eng. Des. (2007), doi:10.1016/j.nucengdes.2007.03.022.
[28] S. Hagen, P. Hofmann, G. Schanz, L. Sepold, in: Proceedings of the 26th National Heat Transfer Conference, Philadelphia, Pennsylvania, 6–9 August 1989, AIChE Symposium Series, vol. 85, 1989, p. 269.
[29] P. Hofmann, S. Hagen, V. Noack, G. Schanz, L. Sepold, Nucl. Technol. 118 (1997) 200.
[30] M.F. Osborne, J.L. Collins, R.A. Lorenz, Nucl. Technol. 78 (1987) 157.
[31] M.F. Osborne, R.A. Lorenz, Nucl. Safety 33 (1992) 344.
[32] J.P. Leveque, B. Andre, G. Ducros, G. Le Marois, G. Lhiaubet, Nucl. Technol. 108 (1994) 33.
[33] B. Andre, G. Ducros, J.P. Leveque, D. Maro, M.F. Osborne, R.A. Lorenz, Nucl. Technol. 114 (1996) 23.
[34] B.J. Lewis, B. Andre, B. Morel, P. Dehaudt, D. Maro, P.L. Purdy, D.S. Cox, F.C. Iglesias, M.F. Osborne, R.A. Lorenz, J. Nucl. Mater. 227 (1995) 83.
[35] F.C. Iglesias, B.J. Lewis, P.J. Reid, P. Elder, J. Nucl. Mater. 270 (1999) 21.
[36] G. Ducros, P.P. Malgouyres, M. Kissane, D. Boulaud, M. Durin, Nucl. Eng. Des. 208 (2001) 191.
[37] Y. Pontillon, P.P. Malgouyres, G. Ducros, G. Nicaise, R. Dubourg, M. Kissane, M. Baichi, J. Nucl. Mater. 344 (2005) 265.
[38] T. Kudo, A. Hidaka, T. Nakamura, H. Uetsuka, J. Nucl. Sci. Technol. 38 (10) (2001) 910.
[39] T. Kudo, T. Nakamura, M. Kida, T. Fuketa, in: Technical Meeting on Severe Accident and Accident Management, Tokyo, Japan, 14–16 March 2006.
[40] D.A. Petti, Nucl. Technol. 84 (1989) 128.
[41] P. Hofmann, S.J.L. Hagen, G. Schanz, A. Skokan, Nucl. Technol. 87 (1989) 146.
[42] R.R. Hobbins, D.A. Petti, D.J. Osetek, D.L. Hagrman, Nucl. Technol. 95 (1991) 287.
[43] A.W. Cronenberg, Nucl. Technol. 93 (1991) 221.
[44] A.W. Cronenberg, Nucl. Technol. 97 (1992) 97.
[45] R.R. Hobbins, D.A. Petti, D.L. Hagrman, Nucl. Technol. 101 (1993) 270.
[46] D.A. Petti, R.R. Hobbins, D.L. Hagrman, Nucl. Technol. 105 (1994) 334.
[47] P. Hofmann, J. Nucl. Mater. 270 (1999) 194.
[48] R.R. Hobbins, D.J. Osetek, D.A. Petti, D.L. Hagrman, in: Proceedings of the ICHMT Conference on Fission Product Transport Processes in Reactor Accidents, Dubrovnik, Yugoslavia, 22–26 May 1989, Hemisphere, New York, 1990, p. 215.
[49] R.R. Hobbins, D.J. Osetek, in: Proceedings of the ICHMT Seminar on Heat and Mass Transfer in Severe Nuclear Reactor Accidents, Cesme, Turkey, 21–26 May 1995, Begell House, New York, 1996, p. 178.
[50] C. Gonnier, G. Repetto, G. Geoffroy, in: W. Krischer, M.C. Rubinstein (Eds.), The Phebus Fission Product Project, Elsevier Applied Science, New York, 1992, p. 108.
[51] M.S. Veshchunov, V.D. Ozrin, V.E. Shestak, V.I. Tarasov, R. Dubourg, G. Nicaise, Nucl. Eng. Des. 236 (2006) 179.
[52] M.S. Veshchunov, R. Dubourg, V.D. Ozrin, V.E. Shestak, V.I. Tarasov, J. Nucl. Mater. 362 (2007) 327.
[53] F. Martín-Fuertes, R. Barbero, J.M. Martín-Valdepeñas, M.A. Jiménez, Nucl. Eng. Des. 237 (2006) 509.
[54] R.D. Gasser, R.O. Gauntt, S. Bourcier, Late-phase Melt Progression Experiment: MP-1: Results and Analysis, NUREG/CR-5874, 1996.
[55] R.D. Gasser, R.O. Gauntt, S. Bourcier, Late-phase Melt Progression Experiment: MP-2: Results and Analysis, NUREG/CR-6167, 1996.
[56] L. Sepold, P. Hofmann, W. Leiling, A. Miassoedov, D. Piel, L. Schmidt, M. Steinbrueck, Nucl. Eng. Des. 204 (1–3) (2001) 205.
[57] P. Hofmann et al., Experiments on the Quench Behaviour of Fuel Rods, 1995 Annual Report on the Project of Nuclear Safety Research, Forschungscentrum Karlsruhe Report FZK-5780, 1996.
[58] Z. Hozer, in: EUROSAFE Berlin 2002: International Forum for Nuclear Safety – Safety Problems in Nuclear Engineering and Nuclear Waste Management, Berlin, Germany, 4–5 November 2002.
[59] Z. Hozer, L. Maroti, P. Windberg, L. Matus, I. Nagy, G. Gyenes, M. Horvath, A. Pinter, M. Balasko, A. Czitrovszky, P. Jani, A. Nagy, O. Prokopiev, B. Toth, Nucl. Technol. 154 (2006) 302.
[60] R.D. MacDonald, J.W. DeVaal, D.S. Cox, L.W. Dickson, M.G. Jonckheere, C.E. Ferris, N.A. Keller, S.L. Wadsworth, in: Proceedings of the Thermal Reactor Safety Meeting, Portland, Oregon, July 1991, also released as an AECL Report AECL-10464, October 1991.

[61] J.W. DeVaal, N.K. Popov, R.D. MacDonald, L.W. Dickson, R.J. Dutton, D.S. Cox, M.G. Jonckheere, in: Proceedings of the Third International Conference on CANDU Fuel, Pembroke, Ontario, Canada, October 1992, also released as AECL Report AECL-10758, March 1993.
[62] L.W. Dickson, P.H. Elder, J.W. DeVaal, J.D. Irish, A.R. Yamazaki, in: Proceedings of the Canadian Nuclear Society 1995 Annual Conference, Saskatoon, Saskatchewan, Canada, June 1995.
[63] L.W. Dickson, J.W. DeVaal, J.D. Irish, P.H. Elder, M.G. Jonckheere, A.R. Yamazaki, in: Proceedings of the Fourth International Conference on CANDU Fuel, Pembroke, Ontario, Canada, October 1995.
[64] R.S. Dickson, L.W. Dickson, Presented at Third OECD Specialist Meeting on Nuclear Aerosols in Reactor Safety, Cologne, Germany, 15–18 June 1998.
[65] J.W. DeVaal, J.D. Irish, L.W. Dickson, S.T. Craig, M.G. Jonckheere, L.R. Bourque, in: Proceedings of the Fifth International Conference on CANDU Fuel, Toronto, 21–25 September 1997.
[66] P.J. Valliant, J.D. Irish, S.T. Craig, in: Proceedings of the Sixth International Conference on CANDU Fuel, Niagara Falls, Canada, 26–29 September 1999.
[67] J.D. Irish, S.T. Craig, L.R. Bourque, M.G. Jonckheere, G. Kyle, P.J. Valliant, L.W. Dickson, R.T. Peplinskie, in: Proceedings of the 19th Annual Conference of the Canadian Nuclear Society, Toronto, 18–21 October 1998.
[68] J.D. Irish, S.T. Craig, P.J. Valliant, in: Proceedings of the Sixth International Conference on CANDU Fuel, Niagara Falls, Canada, 26–29 September 1999.
[69] R.A. Lorenz, M.F. Osborne, A summary of ORNL fission product release tests with recommended release rates and diffusion coefficients, NUREG/CR-6261, ORNL/TM-12801, July 1995.
[70] D.S. Cox, C.E.L. Hunt, Z. Liu, N.A. Keller, R.D. Barrand, R.F. O'Connor, F.C. Iglesias, Presented at the American Nuclear Society International Topical Meeting on the Safety of Thermal Reactors, Portland, Oregon, USA, 21–25 July 1991.
[71] T. Kudo, in: International VERCORS Seminar, Greoux les Bains, France, 15–16 October 2007.
[72] A. Hidaka, T. Kudo, T. Nakamura, H. Uetsuka, Nucl. Sci. Technol. 37 (2002) 759.
[73] A. Hidaka, T. Kudo, T. Nakamura, H. Uetsuka, Nucl. Sci. Technol. 39 (2002) 273.
[74] A. Hidaka, T. Kudo, J. Ishikawa, T. Fuketa, Nucl. Sci. Technol. 42 (2005) 151.
[75] T. Kudo, M. Kida, T. Nakamura, F. Nagase, T. Fuketa, Nucl. Sci. Technol. 44 (2007) 1421.
[76] T. Kudo, M. Kida, T. Nakamura, F. Nagase, T. Fuketa, Nucl. Sci. Technol. 44 (2007) 1428.
[77] D.S. Cox, R.F. O'Connor, W.W. Smeltzer, Solid State Ionics 53-56 (1992) 238.
[78] C.E.L. Hunt, F.C. Iglesias, D.S. Cox, N.A. Keller, R.D. Barrand, J.R. Mitchell, R.F. O'Connor, in: Proceedings of the International Conference on CANDU Fuel, Chalk River, Ontario, Canada, 6–8 October 1986, p. 508.
[79] D.S. Cox, Z. Liu, R.S. Dickson, P.H. Elder, in: Proceedings of the Third International Conference on CANDU Fuel, Chalk River, Canada, 4–8 October 1992.
[80] R.S. Dickson, Z. Liu, D.S. Cox, N.A. Keller, R.F. O'Connor, R.D. Barrand, in: Proceedings of the 15th Annual Canadian Nuclear Society Conference, Montreal, Quebec, 5–8 June 1994.
[81] D.S. Cox, C.E.L. Hunt, Z. Liu, F.C. Iglesias, N.A. Keller, R.D. Barrand, R.F. O'Connor, in: Proceedings of the 12th Annual Conference Canadian Nuclear Society, Saskatoon, Saskatchewan, 1991.
[82] D.S. Cox, Z. Liu, P.H. Elder, C.E.L. Hunt, V.I. Arimescu, Fission-Product Release Kinetics from CANDU and LWR Fuel During High-Temperature Steam Oxidation Experiments, Fission Gas Release and Fuel Rod Chemistry Related to Extended Burnup, IAEA-TECDOC-697, 1993.
[83] Z. Liu, D.S. Cox, R.S. Dickson, P.H. Elder, in: Proceedings of the 15th Annual Canadian Nuclear Society Conference, Montreal, Quebec, 5–8 June 1994.
[84] R.D. Barrand, R.S. Dickson, Z. Liu, D.D. Semeniuk, in: Proceedings of the Sixth International Conference on CANDU Fuel, Niagara Falls, Canada, 26–29 September 1999.
[85] D.S. Cox, C.E.L. Hunt, R.F. O'Connor, R.D. Barrand, F.C. Iglesias, in: Proceedings of the International Symposium on High Temperature Oxidation and Sulphidation Process, Hamilton, Ontario, Canada, 26–30 August 1990, Pergamon, New York, ISBN 0-18-040415-4.
[86] F.C. Iglesias, C.E.L. Hunt, F. Garisto, D.S. Cox, in: Proceedings of the ICHMT Conference on Fission Product Transport Processes in Reactor Accidents, Dubrovnik, Yugoslavia, 22–26 May 1989, Hemisphere, New York, 1990, p. 187.
[87] R.S. Dickson, A.I. Belov, R.D. Barrand, D.D. Semeniuk, M.D. Gauthier, R.T. Peplinskie, S. Yatabe, in: Ninth International Conference on CANDU Fuel, Belleville, Ontario, Canada, 18–21 September 2005.
[88] A.I. Belov, R.S. Dickson, R.T. Peplinskie, M.D. Gauthier, in: Proceedings of the 27th Annual CNS Conference, Toronto, Ontario, Canada, 11–14 June 2006.
[89] G.W. Parker, G.E. Creek, A.L. Sutton, in: Proceedings of the International Meeting on Thermal Nuclear Reactor Safety, Chicago, Illinois, 29 August–2 September 1982, NUREG/CP-0027, vol. 2, US Nuclear Regulatory Commission, 1982.
[90] B.R. Bowsher, R.A. Jenkins, A.L. Nichols, N.A. Rowe, J.A.H. Simpson, Silver-Indium-Cadmium Control Rod Behavior During a Severe Reactor Accident, AEEW-R-1991, UK Atomic Energy Establishment, Winfrith, April 1986.
[91] P. Hofmann, M. Markiewicz, J. Nucl. Mater. 209 (1994) 92.
[92] R.W. Wright, S.J.L. Hagen, in: W. Krischer, M.C. Rubinstein (Eds.), The Phebus Fission Product Project, Elsevier Applied Science, New York, 1992, p. 49.
[93] W. Dienst, P. Hofmann, D. Kerwin-Peck, Nucl. Technol. 65 (1984) 109.
[94] P. Hofmann, H. Uetsuka, A.N. Wilhelm, E.A. Garcia, in: Proceedings of the IAEA/OECD International Symposium on Severe Accidents in Nuclear Power Plants, Sorrento, Italy, IAEA-SM-296/99, 21–25 March 1988, p. 3.
[95] P. Nikolopoulos, P. Hofmann, D.K. Kerwin-Peck, J. Nucl. Mater. 124 (1984) 106.
[96] K.Y. Kim, D.R. Olander, J. Nucl. Mater. 154 (1988) 85.
[97] P.J. Hayward, I.M. George, J. Nucl. Mater. 208 (1994) 35.
[98] P.J. Hayward, I.M. George, J. Nucl. Mater. 208 (1994) 43.
[99] P.J. Hayward, I.M. George, J. Nucl. Mater. 232 (1996) 1.
[100] P.J. Hayward, I.M. George, J. Nucl. Mater. 232 (1996) 13.
[101] M.S. Veshchunov, P. Hofmann, A.V. Berdyshev, J. Nucl. Mater. 231 (1996) 1.
[102] D.W. Akers, R.K. McCardell, Nucl. Technol. 87 (1989) 214.
[103] R.R. Hobbins, M.L. Russell, C.S. Olsen, R.K. McCardell, Nucl. Technol. 87 (1989) 1005.
[104] C.S. Olsen, S.M. Jensen, E.R. Carlson, B.A. Cook, Nucl. Technol. 87 (1989) 57.
[105] B. Clement, private communication, March 2000.
[106] S.M. Jensen, D.W. Akers, B.A. Pregger, Postirradiation Examination Data and Analysis for OECD LOFT Fission Product Experiment LP-FP-2, OECD LOFT-T-3810, vol. 1, Organization of Economic Cooperation and Development, December 1989.
[107] R.R. Hobbins, G.D. McPherson, in: Proceedings of the Open Forum on the OECD/LOFT Project, Achievements and Significant Results, Madrid, Spain, 9–11 May 1990, Organization of Economic Cooperation and Development, 1991.
[108] R. Dubourg, P. Taylor, J. Nucl. Mater. 294 (2001) 32.
[109] I. Johnson, C.E. Johnson, J. Nucl. Mater. 154 (1988) 67.
[110] B.R. Bowsher, S. Dickinson, R.A. Gomme, R.A. Jenkins, A.L. Nichols, J.S. Ogden, in: Proceedings of the Workshop on Chemical Reactivity of Oxide Fuel and Fission product Release, Gloucestershire, England, Central Electricity Generating Board, 7–9 April 1987, p. 455.
[111] R. De Boer, E.H.P. Cordfunke, J. Nucl. Mater. 240 (1997) 124.
[112] R. De Boer, E.H.P. Cordfunke, J. Nucl. Mater. 223 (1995) 103.
[113] J.L. Collins, M.F. Osborne, R.A. Lorenz, Nucl. Technol. 77 (1987) 18.
[114] B.J. Lewis, B. Andre, G. Ducros, D. Maro, Nucl. Technol. 116 (1996) 34.
[115] B.J. Lewis, B.J. Corse, W.T. Thompson, M.H. Kaye, F.C. Iglesias, P. Elder, R. Dickson, Z. Liu, J. Nucl. Mater. 252 (1998) 235.
[116] H. Albrecht, H. Wild, in: Proceedings of the Topl. Mtg. Fission product Behavior and Source Term Research, Snowbird, Utah, 15–19 July 1984, NP-4113-SR, P. 3-1, Electric Power Research Institute , July 1985.
[117] D.R. Olander, J. Nucl. Mater. 270 (1999) 187.
[118] P.R. McClure, M.T. Leonard, A. Razani, Nucl. Sci. Eng. 114 (1993) 102.
[119] L. Väth, Nucl. Technol. 98 (1992) 44.